

The Effect of Stochasticity in Score-Based Diffusion Sampling: a KL Divergence Analysis

Bernardo P. Schaeffer^a, Ricardo M. S. Rosa^a, and Glauco Valle^a

^aInstituto de Matemática, Universidade Federal do Rio de Janeiro

June 16, 2025

Abstract

Sampling in score-based diffusion models can be performed by solving either a probability flow ODE or a reverse-time stochastic differential equation (SDE) parameterized by an arbitrary stochasticity parameter. In this work, we study the effect of stochasticity on the generation process through bounds on the Kullback-Leibler (KL) divergence and complement the analysis with numerical and analytical examples. Our results apply to general forward SDEs with additive noise and Lipschitz-continuous score functions, and quantify how errors from the prior distribution and score approximation propagate under different choices of the stochasticity parameter. The theoretical bounds are derived using log-Sobolev inequalities for the marginals of the forward process, which enable a more effective control of the KL divergence decay along sampling. For exact score functions, we find that stochasticity acts as an error-correcting mechanism, decreasing KL divergence along the sampling trajectory. For an approximate score function, there is a trade-off between error correction and score error amplification, so that stochasticity can either improve or worsen the performance, depending on the structure of the score error. Numerical experiments on simple datasets and a fully analytical example are included to illustrate and enlighten the theoretical results.

1 Introduction

Score-based diffusion models are a generative modeling framework based on the fact that the process of a stochastic differential equation (SDE) admits a time-reversal process, given by another SDE which depends on the score of the (forward) distribution [15, 29]. The forward process is used for training, and the reverse process is used for sampling. Since the main interest is in the distribution itself and not in particular paths of the SDE, a whole family of SDEs (i.e. equation (2), with the parameter $\gamma = \gamma(t)$), including an ordinary differential equation (probability flow ODE, corresponding to $\gamma(t) = 0$), can be used for sampling. In this work, we estimate the evolution, along the sampling process, of the Kullback-Leibler divergence (KL divergence), also known as relative entropy, between the generated and the target distributions, as it depends on the free stochasticity parameter of the family of SDEs/ODE, and as it is affected by approximations of the starting sampling distribution (by a known easy-to-sample distribution) and by approximations of the score function (done in the training phase). This partially answers open questions concerning the role of stochasticity in diffusion model sampling [29, 15, 10]. We complement the rigorous theoretical error estimates with numerical experiments on a one-dimensional problem with known exact distribution and score function, a two-dimensional problem, and also with a fully analytical example. In doing so, we shed some light on the influence of these errors and of the different choices of the stochasticity parameter on the quality of the generated distribution.

Diffusion models are currently the state of the art for generative image and video synthesis [24, 5], and are also being used successfully in many scientific and technological applications, such as natural language process [33], text-to-speech synthesis [32], medical imaging [16], time series analysis [19], protein modeling and design [1, 18], bioinformatics [12], global weather forecasting [23], porous media synthesis [22], and more [31]. Despite their remarkable success in applications, precisely evaluating the performance of a generative model presents challenges such as the independent quantification of sample

quality and distribution coverage [26, 13]. Sample quality can be informally defined as the plausibility of generated samples in the context of original data, and distribution coverage as the amount to which the original distribution is captured by the generated distribution. Thus, a metric for sample quality should measure how large the density of the generated distribution is in regions where the density of the target distribution is small, and, conversely, a metric for mode coverage should measure how large is the target density where the generated density is small.

The KL divergence $H(p_1|p_2) := \int p_1 \log(p_1/p_2)$ is a standard statistical measure between probability distributions, which, by its asymmetry, provides two possible metrics to compare a generated distribution \tilde{p} with a target distribution p . Both divergences measure sample quality and distribution coverage, but $H(\tilde{p}|p)$ gives more weight to the former and $H(p|\tilde{p})$ to the latter, as the integrand $p(x) \log p(x)/q(x)$ is large when $q(x) \ll p(x)$, and thus regions of X where $q(x) \ll p(x)$ contribute more to the divergence $H(p|q)$ than to $H(q|p)$. Different applications might be more sensitive to either sample quality or distribution coverage, making both divergences relevant for evaluating a generative model from a theoretical perspective¹. Therefore, in this work we investigate the impact of stochastic sampling in model performance through both divergences, filling a gap in the existing literature on KL divergence bounds for diffusion models, which is more focused on $H(p|\tilde{p})$ (associated with mode coverage) [8, 6, 17, 9] essentially for technical reasons. Moreover, we are able to use log-Sobolev inequalities to derive stronger bounds for $H(\tilde{p}|p)$ (associated with sample quality), while the corresponding bound for $H(p|\tilde{p})$ seems more elusive.

For a (forward) SDE

$$dX_t = f(X_t, t)dt + g(t)dW_t, \quad (1)$$

in \mathbb{R}^n , on a time interval $[0, T]$, with probability density $p_t(x)$, where $f = f(x, t)$ and $g = g(t)$ are given and $\{W_t\}_{t \geq 0}$ is an n -dimensional Wiener process, the associated reverse-time SDE takes the form

$$d\tilde{X}_\tau = \left(-\bar{f}(\tilde{X}_\tau, \tau) + \frac{1}{2}\bar{g}^2(\tau)(1 + \gamma(\tau))\nabla \log \bar{p}_\tau(\tilde{X}_\tau) \right) d\tau + \sqrt{\gamma(\tau)}\bar{g}(\tau)dW_\tau, \quad (2)$$

in the reversed time variable $\tau = T - t$, where $\bar{f}(x, \tau) := f(x, T - \tau)$, $\bar{g}(\tau) := g(T - \tau)$, $\bar{p}_\tau(x) := p_{T - \tau}(x)$, and where $\gamma(\tau) \geq 0$ is arbitrary. It is well known [3, 15] that, under certain conditions, the reverse-time SDE (2) has the same densities of the forward SDE (1) under the change of variables $\tau = T - t$. More precisely, denoting the density associated with (2) by \tilde{p}_τ , if the initial distribution for (2) is $\tilde{p}_0 = \bar{p}_0 = p_T$, then for all $\tau \in (0, T)$ it holds that $\tilde{p}_\tau = \bar{p}_\tau$. A short proof is provided in Section 2.1 for the sake of completeness. Note that (2) gives a family of equations, indexed by the free functional parameter $\gamma(\tau) \geq 0$.

If the (Stein) score function $\nabla \log p(t, \cdot)$ of the forward process given by (1) is known exactly or approximately, for all $0 < t \leq T$, and if at time $t = T$ the distribution p_T is close to a Gaussian distribution or any other distribution which is easy to sample from, the reverse-time SDE (2) can then be used as a generic sampler for p_0 . In practice, the score function $\nabla \log p(t, \cdot)$ can be approximated by a neural network $s_\theta(t, \cdot)$ trained with denoising score-matching [30, 15]. Then, sampling is performed via the approximate reverse-time SDE

$$d\tilde{X}_\tau = \left(-\bar{f}(\tilde{X}_\tau, \tau) + \frac{1}{2}\bar{g}^2(\tau)(1 + \gamma(\tau))\bar{s}_\theta(\tau, \tilde{X}_\tau) \right) d\tau + \sqrt{\gamma(\tau)}\bar{g}(\tau)dW_\tau, \quad (3)$$

where $\bar{s}_\theta(\tau, x) = s_\theta(t - \tau, x)$ is the reverse-time approximated score. In the machine-learning literature [29], two common choices for γ correspond to setting $\gamma \equiv 0$ (Probability Flow ODE), and $\gamma \equiv 1$ (Anderson/Song's reverse-time SDE).

In summary, the diffusion model algorithm consists of

- (i) choosing an adequate forward process (1) for which p_T is close to a known and easy-to-sample distribution q ;
- (ii) training a score model $s_\theta(t, x)$ to approximate $\nabla \log p_t(x)$, for all $0 < t \leq T$, by minimizing the global loss function \mathcal{L} ;
- (iii) sampling the starting condition \tilde{X}_0 from the prior distribution $q(x) \approx p_T(x)$; and

¹We note that the use of KL divergences as a metric for evaluating a specific trained model is limited, since the densities p, \tilde{p} are not generally available.

- (iv) numerically integrating, from $\tau = 0$ to $\tau = T$, the approximate reverse-time equation (3) with the starting condition \tilde{X}_0 .

This pipeline generates a final sample $\tilde{X}_T \sim \tilde{p}_T$, and it is desired that \tilde{p}_T be as close as possible to p_0 , the unknown data distribution. Its main sources of error are

- (E1) approximation errors of the score function in the training phase;
- (E2) approximation errors of the starting prior distribution p_T in the sampling phase;
- (E3) numerical integration errors of the sampling process.

This work studies the sampling part of the diffusion algorithm, focusing on the effect of the free parameter γ on the correction and propagation of errors from sources (E1) and (E2). The choice of the integration scheme for solving (3) and the associated numerical errors are also of great importance, but these are not our focus here. Thus, for the theoretical results, we consider the exact solution of either (2) or (3), focusing only on errors (E1) and (E2), while for the numerics we simply use Euler and Euler-Maruyama schemes with a very fine time mesh.

Our work is inspired by a conjecture in Karras et al [15] about the role of stochasticity in equation (2) and by the approach of Markowich and Villani [20] to prove convergence to the stationary distribution for the overdamped Langevin equation. The conjecture is that stochasticity, i.e. a strictly positive $\gamma(t)$, can act as a Langevin-like corrector directing the reverse-time densities \tilde{p}_τ closer to the true forward distributions p_t . There are many ways to prove convergence towards the stationary distribution of the overdamped Langevin equation, and the work in [20] seems to be one of the simplest and most natural, using a logarithmic Sobolev inequality (LSI) to obtain a bound which decreases exponentially in the time variable. Our first results (Section 3.1) formalize and proves the conjecture in [15] by adapting the approach in [20] to the reverse-time SDEs (2), while in Section 3.2 we extend these results to the approximate reverse-time SDE (3).

In Section 3.1, we consider the SDE (2) with an exact score function and approximate starting prior, addressing the source of error (E2). In this case, the KL divergence estimate explicitly demonstrates the advantage of stochasticity, confirming the conjecture in [15]. Next, in Section 3.2, we consider the more realistic setting of an approximate score function $s(x, t) = \nabla \log p_t(x, t) + \epsilon(x, t)$, where $\epsilon = \epsilon(x, t)$ is the associated error, addressing both errors (E2) and (E1). Here, stochasticity still produces a correction term in the evolution of the generated distribution, but it also amplifies the score error ϵ by a multiplicative factor, making its overall impact more subtle. This behavior reflects empirical findings reported in [10, 15], where the relative performance of stochastic and deterministic sampling varies significantly depending on the dataset and training regime.

More precisely, we prove in Theorem 3, under suitable conditions, a formula for the evolution of the relative entropy which can be also found in previous works [6, 2] relying on formal arguments. This is given by

$$\frac{d}{d\tau} H(\tilde{p}_\tau | \bar{p}_\tau) = \frac{1}{2} \bar{g}^2 (1 + \gamma) \int \epsilon \cdot \left(\nabla \log \frac{\tilde{p}_\tau}{\bar{p}_\tau} \right) \tilde{p}_\tau dx - \frac{1}{2} \gamma \bar{g}^2 \int \left| \nabla \log \frac{\tilde{p}_\tau}{\bar{p}_\tau} \right|^2 \tilde{p}_\tau dx,$$

where $H(p_1 | p_2) := \int p_1(x) \log(p_1(x)/p_2(x)) dx$ is the KL divergence, or relative entropy, of p_1 with respect to p_2 . Then, if \bar{p}_τ satisfies a log-Sobolev inequality (8) with constant $C(\tau)$, Theorem 4 provides in equation (23) the entropy estimate

$$H(\tilde{p}_\tau | \bar{p}_\tau) \leq e^{-\int_0^\tau a(s) ds} H(\tilde{p}_0 | \bar{p}_0) + \frac{1}{2} \int_0^\tau \bar{g}(s)^2 (1 + \gamma(s)) E_{\tilde{p}_s} [\epsilon_s \cdot \nabla \log h_s] e^{-\int_s^\tau a(r) dr} ds,$$

where $a(s) = C(s)^{-1} \gamma(s) g(s)^2$ and $h_s = \tilde{p}_s / \bar{p}_s$. When γ is strictly positive, a more explicit estimate is given by equation (24), which eliminates the explicit dependence on $\nabla \log h$ and depends on ϵ only through its $L^2(\tilde{p})$ norm.

The case of exact score functions is addressed by Theorems 1 and 2, where one clearly sees that the larger the γ the faster the convergence. However, this makes the problem stiff, adding an effective faster time scale to the dynamics. In practice, this poses a challenge to the numerical approximation of the problem, limiting the choice of γ , as discussed in Section 3.1.1.

In Section 4, we test the theoretical bounds in numerical experiments, comparing with estimated values for the relative entropy. This is done for 1D and 2D Gaussian mixture data distributions, for

which accurate entropy estimation is feasible, the score functions are known analytically, and we can also visually compare generated and data distributions. We consider both exact and approximate scores learned by a simple MLP, and investigate the trade-off between score errors and accumulated errors suggested by the bounds in Section 3.2. In particular, a grid search for the best interval to include stochasticity supports our theoretical considerations in Remark 3.2. Since, even for simple datasets, reliably estimating $\nabla \log \tilde{p}$ is not straightforward, we conclude by presenting in Section 5 a fully analytical example, based on a single Gaussian dataset, where it is possible to explicitly compare the KL divergence with the first bound of Theorem A.2.

1.1 Related work

There is a large body of recent work that studies convergence bounds for score-based diffusion models. The results obtained by [6] and [9] are the closest to ours, also obtaining bounds in the KL divergence, albeit for $H(p_{\text{data}}|p_{\text{generated}})$ instead of $H(p_{\text{generated}}|p_{\text{data}})$. This difference is due to their use of LSIs for the Gaussian measure, in the forward process, for bounding the prior approximation error, while we use LSIs for the marginals p_t in the sampling process, to account for the entropy decrease induced by the SDE. Therefore, these works focus mainly on bounding errors arising from prior and score approximation, and discretization, without explicitly quantifying the differences between deterministic and stochastic sampling. There is some overlap in the proof techniques; for example, our Lemma 3.1 is Lemma C.1 in [6].

The results in [2, Section 2.4] are an important extension of the bounds for $H(p_{\text{data}}|p_{\text{generated}})$, previously known in the literature for specific choices of forward process, to very general ones. Moreover, [2] also consider the general reverse SDE with free parameter $\gamma(t)$, and establish an advantage of the reverse SDEs over the flow ODE, given by the fact that the KL divergence of a distribution generated by an SDE is bounded by the score-matching error. Thus, score-matching training effectively minimizes the KL divergence for SDE sampling (even though the bound might still be very large), while the same is not ensured for ODE sampling. A similar result was previously obtained by [28] for the reverse SDE with $\gamma = 1$.

Despite the commonalities, our work has the essentially distinct objective of studying the effect of stochasticity in diffusion sampling. Our main contribution consists of using log-Sobolev inequalities for $\nabla \log p_t$ to incorporate an explicit decrease factor in KL divergence along sampling, which can be found in Theorem 4. In the absence of score approximation errors, this results in a decrease in the final entropy; see Theorem 2. We observe that a similar decrease has previously been studied for other metrics, as, for example, in [17]. Moreover, we believe that our numerical experiments, together with the analytical example, can shed light on this phenomenon and orient future research.

Another contribution is to explicitly investigate the conditions required by this kind of bound, without relying on formal arguments. As stated in Corollary 3.1, these are automatically satisfied by forward processes with a null drift term (such as the EDM and VE processes of [15] and [29]), if the data distribution p_0 has compact support, as in the case of image data. The more general conditions are stated in the Theorems, and require that the diffused data distributions p_t satisfy a log-Sobolev inequality. We note that, although compact support with null drift is sufficient to ensure the log-Sobolev condition, the tightness of the bound actually depends on the log-Sobolev constant obtained.

2 Background

Here, we mention some preliminary results to be used in the next sections. See the Appendix A for proofs and more details.

2.1 Reverse-time SDEs

Let

$$dX_t = f(X_t, t) + g(t)dW_t, \tag{4}$$

be an SDE for which there exists a unique solution² in the interval $[0, T]$, and let p_t be its associated density, i.e. the solution of the associated Fokker-Planck (FP) equation

$$\frac{\partial p}{\partial t} = -\nabla \cdot (fp) + \frac{1}{2}g^2\Delta p. \quad (5)$$

As mentioned earlier, we extensively use the following result, which also can also be found in [15][Appendix B.5]. See also [3, 29].

Lemma 2.1 (Reverse-time formula). *Consider the family of SDEs given by*

$$d\tilde{X}_\tau = \left(-\bar{f}(\tilde{X}_\tau, \tau) + \frac{1}{2}\bar{g}^2(\tau)(1 + \gamma(\tau))\nabla \log \bar{p}_\tau(\tilde{X}_\tau) \right) d\tau + \sqrt{\gamma(\tau)}\bar{g}(\tau)dW_\tau, \quad (6)$$

for $\tau \in [0, T]$, where $\gamma(\tau)$ is an arbitrary non-negative function, and $\bar{f}(x, \tau) := f(x, T - \tau)$, $\bar{g}(\tau) := g(T - \tau)$ and $\bar{p}_\tau(x) := p_{T-\tau}(x)$. Denote by \tilde{p}_τ^γ its associated probability densities. If the initial density is $\tilde{p}_0 = \bar{p}_0 = p_T$, then the densities \tilde{p}_τ^γ are independent of γ , and we have $\tilde{p}_\tau = p_{T-\tau}$. Since (6) is an SDE in reverse-time that has the same densities of (4), we call it a **reverse-time SDE** associated with (4).

2.2 Logarithm-Sobolev Inequalities (LSI)

Definition. Given μ a probability measure in \mathbb{R}^n , define the entropy functional as $Ent_\mu(f^2) := \int f^2 \log f^2 d\mu - (\int f^2 d\mu) \log (\int f^2 d\mu)$. Then, μ is said to satisfy a logarithmic Sobolev inequality (LSI) with constant C if

$$Ent_\mu(f^2) \leq 2C \int \|\nabla f\|^2 d\mu \quad (7)$$

for any smooth function f .

Lemma 2.2. Condition (7) implies that μ satisfies

$$H(\tilde{\mu}|\mu) \leq \frac{C}{2} \int \left| \nabla \log \frac{d\tilde{\mu}}{d\mu} \right|^2 d\tilde{\mu} \quad (8)$$

for all probability measures $\tilde{\mu}$ for which the Radom-Nikodym derivative $d\tilde{\mu}/d\mu$ is smooth.

For the remainder of the text, we use the LSIs in the form of equation (8).

3 KL divergence bounds

It is well known that the probability densities $q_t(x)$ associated to the time-independent Langevin equation

$$dX_t = \nabla \log \pi(X_t)dt + \sqrt{2}dW_t$$

converge to the stationary distribution π when $t \rightarrow \infty$ [25]. It is also known [20] that, under some conditions on the target distribution π , the distribution q_t converge to π exponentially in the KL divergence. More specifically, there is the exponential bound

$$H(q_t|\pi) \leq e^{-Ct}H(q_0|\pi), \quad (9)$$

where $H(q|p) := \int \log \frac{q}{p} q dx$ is the KL divergence and $C = C(\pi) > 0$ is constant in t . Thus, deviations in the initial distribution are corrected over time by the Langevin diffusion.

Aggregating the terms with γ in the reverse-time SDE (6), we can write it as

$$d\tilde{X}_\tau = \left(-\bar{f}(\tilde{X}_\tau, \tau) + \frac{1}{2}\bar{g}^2(\tau)\nabla \log \bar{p}_\tau(\tilde{X}_\tau) \right) d\tau + \left(\frac{1}{2}\bar{g}^2(\tau)\gamma(\tau)\nabla \log \bar{p}_\tau(\tilde{X}_\tau)d\tau + \sqrt{\gamma(\tau)}\bar{g}(\tau)dW_\tau \right). \quad (10)$$

²As, for example, in the case where f, g are globally Lipschitz.

Inspired by this form, in [15, Section 4] it is proposed that the reverse-time SDE should be seen as a Probability Flow ODE, i.e. the reverse-time SDE with $\gamma \equiv 0$, with the addition of a Langevin-like error-correcting term. This suggests that a bound similar to (9) might be found for the reverse-time SDE.

In this section, we make this idea precise, studying the KL divergence of the densities \tilde{p}_τ of the reverse-time SDE with some initial density \tilde{p}_0 with respect to the probability densities \bar{p}_τ of the reverse-time SDE with initial density $\bar{p}_0 = p_T$, which, by Lemma 2.1, corresponds to the densities of the forward SDE. In 3.1, we obtain a result analogous to (9), with \bar{p}_τ assuming the role of the stationary distribution π . Section 3.2 studies the more general case of an approximated reverse-time SDE, in which $\nabla \log \bar{p}_\tau(x)$ is replaced by $s(x, \tau) := \nabla \log \bar{p}_\tau(x) + \epsilon(x, \tau)$, for an approximation error $\epsilon(x, \tau)$.

We will use the following general lemma, which can also be found in [6, Lemma C.1].

Lemma 3.1. *Let p_t and q_t be solutions of the Fokker-Planck equations associated to the SDEs in \mathbb{R}^n*

$$\begin{aligned} dX_t &= a_1(X_t, t)dt + b(t)dW_t^{(1)} \\ dY_t &= a_2(Y_t, t)dt + b(t)dW_t^{(2)}, \end{aligned}$$

where $W^{(1)}$ and $W^{(2)}$ are two independent n -dimensional Wiener processes. If $p_t, q_t, \nabla p$ and ∇q have a super-polynomial decay, and the coefficients $a_1(t), a_2(t), b(t)$ are C^1 and grow at most polynomially, then the evolution of the relative entropy $H(p_t|q_t)$ is given by

$$\frac{d}{dt}H(p_t|q_t) = -\frac{1}{2}b^2(t) \int \left| \nabla \log \frac{p_t}{q_t} \right|^2 p_t dx + \int (a_1 - a_2) \cdot \left(\nabla \log \frac{p_t}{q_t} \right) p_t dx. \quad (11)$$

3.1 Prior distribution approximation errors

In this section, we include only the approximation error in the initial condition, that is, the setting where \tilde{p}_τ and \bar{p}_τ are solutions of (2) for given initial conditions \tilde{p}_0 and $\bar{p}_0 = p_T$.

Using Lemma 3.1 for \tilde{p}_τ and \bar{p}_τ , with $a_1 = a_2$, we obtain the following result.

Theorem 1. *Let \bar{p}_τ and \tilde{p}_τ be as previously defined, and let $\tau \in (0, T)$. If the function $x \mapsto \bar{p}_\tau(x)$ has sub-Gaussian tails³ and $\nabla \log \bar{p}_\tau$ is Lipschitz, then the evolution of the KL divergences between \tilde{p}_τ and \bar{p}_τ is given by*

$$\frac{d}{dt}H(\tilde{p}_\tau|\bar{p}_\tau) = -\frac{1}{2}\gamma(\tau)\bar{g}^2(\tau) \int \left| \nabla \log \frac{\tilde{p}_\tau}{\bar{p}_\tau} \right|^2 \tilde{p}_\tau dx \quad (12)$$

and

$$\frac{d}{dt}H(\bar{p}_\tau|\tilde{p}_\tau) = -\frac{1}{2}\gamma(\tau)\bar{g}^2(\tau) \int \left| \nabla \log \frac{\tilde{p}_\tau}{\bar{p}_\tau} \right|^2 \bar{p}_\tau dx. \quad (13)$$

Theorem 1 shows that the KL divergence decreases in $\tau \in (0, T)$ if and only if there is an open interval $(a, b) \subset (0, \tau)$ such that $\gamma(s) > 0$ for $s \in (a, b)$. If $\gamma \equiv 0$, which is the case for the Probability Flow ODE, the entropy remains constant for $\tau \in (0, T)$.

However, this result alone is not sufficient to quantify the final entropy decrease due to the dependence on the unknown \tilde{p}_τ . This dependence can be eliminated through the use of a logarithmic Sobolev inequality.

Theorem 2. *Let $\bar{p}_\tau, \tilde{p}_\tau$ be as before. If \bar{p}_τ satisfies a log-Sobolev inequality with constant $C(\tau)$ and $\nabla \log \bar{p}_\tau$ is Lipschitz for all $\tau \in (0, T)$, then we have the following decay estimate on the KL divergence*

$$H(\tilde{p}_\tau|\bar{p}_\tau) \leq e^{-\int_0^\tau C(s)^{-1}\gamma(s)\bar{g}(s)^2 ds} H(\tilde{p}_0|\bar{p}_0) \quad (14)$$

for all $\tau \in (0, T)$, and also for $\tau = T$ if \tilde{p}_T is absolutely continuous with respect to \bar{p}_T .

A corresponding result holds for $H(\bar{p}_\tau|\tilde{p}_\tau)$ if \tilde{p}_τ satisfies an LSI.

³i.e. if there are constants $C = C(\tau)$ and $c = c(\tau)$ such that $\bar{p}_\tau(x) \leq Ce^{-c|x|^2}$.

Proof. Since \bar{p}_τ satisfies an LSI, it has sub-Gaussian tails (see, for example, [4]). Thus, by Theorem 1, equation (12) gives that for all $\tau \in (0, T)$

$$\frac{d}{dt}H(\tilde{p}_\tau|\bar{p}_\tau) = -\frac{1}{2}\gamma(\tau)g(\tau) \int \left| \nabla \log \frac{\tilde{p}_\tau}{\bar{p}_\tau} \right|^2 \tilde{p}_\tau dx.$$

Now, explicitly using the inequality (8), we have

$$\frac{d}{d\tau}H(\tilde{p}_\tau|\bar{p}_\tau) = -\frac{1}{2}\gamma(\tau)g(\tau)^2 \int \left| \nabla \log \frac{\tilde{p}_\tau}{\bar{p}_\tau} \right|^2 \tilde{p}_\tau dx \leq -\frac{1}{C(\tau)}\gamma(\tau)g(\tau)^2 H(\tilde{p}_\tau|\bar{p}_\tau).$$

and by Grönwall's inequality we obtain (14). \square

Remark 3.1. *By the Csiszár-Kullback inequality, which gives $\|p_1 - p_2\|_{\mathcal{L}^1} \leq 2H(p_1|p_2)$, Theorem 2 gives a corresponding bound on the L^1 distance $\|\tilde{p}_T - p_T\|_{\mathcal{L}^1}$.*

Note that although this result can hold for both $H(\tilde{p}_\tau|\bar{p}_\tau)$ and $H(\bar{p}_\tau|\tilde{p}_\tau)$, it is easier to ensure the condition that \bar{p}_τ satisfies an LSI, than that \tilde{p}_τ does. If $f = 0$, as the EDM and VE processes used in [29, 15], the SDE is linear and the forward densities can be written as $p_t = p_0 * \mathcal{N}(0, \sigma^2(t)I)$, with $\sigma(t)^2 := \int_0^t g(s)^2 ds$. Since in this case p_t is a Gaussian convolution, we know that p_t satisfies an LSI with the following explicit constant.

Corollary 3.1. *If $f \equiv 0$ and $p_0 = \bar{p}_T$ has compact support, with $\text{supp}(p_0) \in B_R(0)$, then $\bar{p}_{T-t} = p_t$ satisfies the hypothesis of Theorem 2 with a dimension-free log-Sobolev constant given by*

$$C(t) = 6(4R^2 + \sigma(s)^2)e^{\frac{4R^2}{\sigma(s)^2}}, \quad (15)$$

where $\sigma(t)^2 := \int_0^t g(s)^2 ds$ (in forward time t).

3.1.1 Remark: the functional parameter γ

Since the bound (14) shows a KL divergence decay which is exponential on the stochasticity parameter γ , what is the disadvantage of setting γ arbitrarily large? The disadvantage is related to the numerical approximation. A simple Euler-Maruyama discretization step of the reverse-time SDE (6) is given by

$$\begin{aligned} X_{\tau_{i+1}} &= X_{\tau_i} + \left(-\bar{f}(X_{\tau_i}, \tau_i) + \frac{1}{2}\bar{g}^2(\tau_i)(1 + \gamma(\tau_i))\nabla \log \bar{p}_{\tau_i}(X_{\tau_i}) \right) \Delta\tau_i + \sqrt{\gamma(\tau_i)\bar{g}(\tau_i)}\sqrt{\Delta\tau_i}\xi \\ &= X_{\tau_i} + \left(-\bar{f}(X_{\tau_i}, \tau_i) + \frac{1}{2}\bar{g}^2(\tau_i)\nabla \log \bar{p}_{\tau_i}(X_{\tau_i}) \right) \Delta\tau_i \\ &\quad + \frac{1}{2}\bar{g}^2(\tau_i)\nabla \log \bar{p}_{\tau_i}(X_{\tau_i})(\gamma(\tau_i)\Delta\tau_i) + \bar{g}(\tau_i)\sqrt{\gamma(\tau_i)\Delta\tau_i}\xi \end{aligned} \quad (16)$$

where $\xi \sim \mathcal{N}(0, 1)$, and $\Delta\tau_i := \tau_{i+1} - \tau_i$. Thus, comparing (16) with (10), one can see that $\gamma(\tau_i)\Delta\tau_i$ gives an effective discretization step size for the Langevin-like part of the reverse SDE. Therefore, setting γ too large will inevitably produce significant discretization errors. In Section 4, we show the trade-off between error correction and discretization errors in numerical experiments; see Figure 3.

3.2 Score approximation errors

The previous bounds can be readily generalized to the case where the reverse-time SDE depends on an approximated score $s(x, \tau) = \nabla \log \bar{p}_\tau(x) + \epsilon_\tau(x)$, for some error function $\epsilon_\tau(x)$. This models the setting of $s(x, \tau)$ being a neural network trained by score-matching, as in the diffusion model algorithm described in the Introduction.

The approximated version of equation (6) is given by

$$d\tilde{X}_\tau = \left(-\bar{f}(\tilde{X}_\tau, \tau) + \frac{1}{2}\bar{g}^2(\tau)(1 + \gamma(\tau)) \left(\nabla \log \bar{p}_\tau(\tilde{X}_\tau) + \epsilon_\tau(\tilde{X}_\tau) \right) \right) d\tau + \sqrt{\gamma(\tau)\bar{g}(\tau)}dW_\tau, \quad (17)$$

with a corresponding Fokker-Planck equation

$$\frac{\partial \tilde{p}}{\partial \tau} = -\nabla \cdot \left(\left(-\bar{f} + \frac{1}{2}\bar{g}^2(\gamma + 1)(\nabla \log \bar{p} + \epsilon) \right) \tilde{p} \right) + \frac{1}{2}\gamma\bar{g}^2\Delta\tilde{p}. \quad (18)$$

Thus, we can use Lemma 3.1 to obtain straightforward generalizations of Theorems 1 and 2.

Theorem 3. Let \bar{p}_τ be as before and \tilde{p}_τ be a solution of the perturbed Fokker-Planck (18) with initial condition \tilde{p}_0 . Under the same hypotheses of Theorem 1, if $\epsilon(\cdot, \tau)$ is differentiable and such that $\epsilon(\cdot, \tau)\tilde{p}_\tau = o(|x|^{n-1})$, we have, for all $\tau \in (0, T)$,

$$\frac{d}{d\tau} H(\tilde{p}_\tau | \bar{p}_\tau) = \frac{1}{2} \bar{g}^2 (1 + \gamma) \int \epsilon \cdot \left(\nabla \log \frac{\tilde{p}_\tau}{\bar{p}_\tau} \right) \tilde{p}_\tau dx - \frac{1}{2} \gamma \bar{g}^2 \int \left| \nabla \log \frac{\tilde{p}_\tau}{\bar{p}_\tau} \right|^2 \tilde{p}_\tau dx, \quad (19)$$

and, provided that $\epsilon(\cdot, t)p_t = o(|x|^{n-1})$, also that

$$\frac{d}{d\tau} H(\bar{p}_\tau | \tilde{p}_\tau) = \frac{1}{2} \bar{g}^2 (1 + \gamma) \int \epsilon \cdot \left(\nabla \log \frac{\tilde{p}_\tau}{\bar{p}_\tau} \right) \bar{p}_\tau dx - \frac{1}{2} \gamma \bar{g}^2 \int \left| \nabla \log \frac{\tilde{p}_\tau}{\bar{p}_\tau} \right|^2 \bar{p}_\tau dx. \quad (20)$$

Proof. Since the hypotheses of Theorem 1 are satisfied, both formulas follow directly from Lemma 3.1 with the assumption on ϵ_t . \square

Remark 3.2. Equation (19) suggests a criterion for choosing $\gamma(t)$ so that the derivative of H at time t is minimized. Note that, since \tilde{p}_{τ_2} also depends on $\gamma(\tau_1)$ if $\tau_2 > \tau_1$, minimizing (19) for each $s < \tau$ might not result in a minimum for the final entropy $H(\tilde{p}_\tau | \bar{p}_\tau)$, but the resulting heuristics can be used as a general guideline. At end of Section 4.2, we show a choice of $\gamma(t)$ motivated by it, together with a case where the mentioned problem occurs.

Writing equation (19) as

$$\frac{d}{d\tau} H(\tilde{p}_\tau | \bar{p}_\tau) = \frac{1}{2} \bar{g}^2 \int \epsilon \cdot \left(\nabla \log \frac{\tilde{p}_\tau}{\bar{p}_\tau} \right) \tilde{p}_\tau dx + \frac{1}{2} \gamma \bar{g}^2 \int \left(\epsilon \cdot \nabla \log \frac{\tilde{p}_\tau}{\bar{p}_\tau} - \left| \nabla \log \frac{\tilde{p}_\tau}{\bar{p}_\tau} \right|^2 \right) \tilde{p}_\tau dx \quad (21)$$

we can see that $dH/d\tau$ is minimized at each τ by setting $\gamma(\tau) = 0$ when the expectation $E_{\tilde{p}_\tau}[\epsilon \cdot \nabla \log(\tilde{p}_\tau/\bar{p}_\tau) - |\nabla \log(\tilde{p}_\tau/\bar{p}_\tau)|^2]$ is non-negative, and to as large as possible, limited by the discretization issues discussed in 3.1.1, when that expectation is negative.

This condition seems to be unverifiable in practice, but since

$$\begin{aligned} \epsilon_\tau(x) \cdot \nabla \log \frac{\tilde{p}_\tau}{\bar{p}_\tau}(x) - \left| \nabla \log \frac{\tilde{p}_\tau}{\bar{p}_\tau}(x) \right|^2 &\leq |\epsilon_\tau(x)| \left| \nabla \log \frac{\tilde{p}_\tau}{\bar{p}_\tau}(x) \right| - \left| \nabla \log \frac{\tilde{p}_\tau}{\bar{p}_\tau}(x) \right|^2 \\ &= \left| \nabla \log \frac{\tilde{p}_\tau}{\bar{p}_\tau}(x) \right| \left(|\epsilon_\tau(x)| - \left| \nabla \log \frac{\tilde{p}_\tau}{\bar{p}_\tau}(x) \right| \right), \end{aligned}$$

$\gamma(\tau)$ should be positive if $|\epsilon_\tau(x)| < |\nabla \log \tilde{p}_\tau(x)/\bar{p}_\tau(x)|$ in expectation with respect to $\tilde{p}_\tau(x)|\nabla \log \tilde{p}_\tau(x)/\bar{p}_\tau(x)|$. Note that an analogous condition for the entropy $H(p_\tau | \bar{p}_\tau)$ follows from equation (20), taking the expectation w.r.t $\bar{p}_\tau(x)|\nabla \log \tilde{p}_\tau(x)/\bar{p}_\tau(x)|$. The fact that $|\nabla \log \tilde{p}_\tau(x)/\bar{p}_\tau(x)|$ is a function of accumulated errors suggests the broad guideline that $\gamma(\tau)$ should be positive when the score approximation error is smaller in expectation than the accumulated errors.

Corollary 3.2. Using Young's inequality on equation (20), we have that, for every positive function $\eta = \eta(t)$,

$$H(\bar{p}_\tau | \tilde{p}_\tau) \leq H(\bar{p}_0 | \tilde{p}_0) + \frac{1}{2} \int_0^\tau \bar{g}^2 \int \left((1 + \gamma)\eta(s)|\epsilon|^2 + \left(\frac{1 + \gamma}{4\eta(s)} - \gamma \right) \left| \nabla \log \frac{\tilde{p}_s}{\bar{p}_s} \right|^2 \right) \bar{p}_s dx ds.$$

In particular, taking $\eta(\tau) = (1 + \gamma(\tau))/4\gamma(\tau)$, it is possible to obtain the explicit bound

$$H(\bar{p}_\tau | \tilde{p}_\tau) \leq H(\bar{p}_0 | \tilde{p}_0) + \frac{1}{8} \int_0^\tau \bar{g}^2 \frac{(1 + \gamma)^2}{\gamma} \left(\int |\epsilon|^2 \bar{p}_s dx \right) ds. \quad (22)$$

A corresponding result for the framework of stochastic interpolants can be found in [2], Lemma 2.22.

Theorem 4. Assume the same hypotheses of Theorem 3. If, for all $s \in (0, \tau)$, \bar{p}_s satisfies a log-Sobolev inequality with constant $C(s)$, and $\nabla \log \bar{p}_s$ is Lipschitz, then we have that

$$H(\tilde{p}_\tau | \bar{p}_\tau) \leq e^{-\int_0^\tau \alpha(s) ds} H(\tilde{p}_0 | \bar{p}_0) + \frac{1}{2} \int_0^\tau \bar{g}(s)^2 (1 + \gamma(s)) E_{\bar{p}_s} [\epsilon_s \cdot \nabla \log h_s] e^{-\int_s^\tau \alpha(r) dr} ds, \quad (23)$$

for $\alpha(s) := C(s)^{-1}\gamma(s)g(s)^2$, where $h_s := \tilde{p}_s/\bar{p}_s$.

Moreover, if $\gamma(s) > 0$ for all $s \in (0, \tau)$, then, for any measurable function $\delta(s)$ satisfying $0 < \delta(s) \leq \gamma(s)$ in $(0, \tau)$, we have

$$H(\tilde{p}_\tau|\bar{p}_\tau) \leq e^{-\int_0^\tau \alpha(s,\delta)ds} H(\tilde{p}_0|\bar{p}_0) + \frac{1}{8} \int_0^\tau \frac{1}{\delta(s)} \bar{g}(s)^2 (1 + \gamma(s))^2 E_{\tilde{p}_s} [|\epsilon_s|^2] e^{-\int_s^\tau \alpha(r,\delta)dr} ds, \quad (24)$$

where $\alpha(s, \delta) := C(s)^{-1}\bar{g}(s)^2(\gamma(s) - \delta(s))$.

Proof. See Appendix A. □

Remark 3.3. 1. In this case, an increase in γ is not clearly related to a decrease in the final entropy.

2. Note that the bound in equation (22) is identical to the one in (24) with $\delta = \gamma$ (that is, ignoring the decay factor), but with the expectation taken in \tilde{p}_τ instead of \tilde{p}_τ .

3. Note in formula (23) that the vector $\nabla \log h_s(x) = \nabla \log \tilde{p}_s(x) - \nabla \log \bar{p}_s(x)$ defines a principal direction for the propagation and correction of errors, which is independent of the choice of $\gamma(t)$. For example, the component of $\epsilon_s(x)$ perpendicular to $\nabla \log h_s(x)$ does not affect the final entropy $H(\tilde{p}_T|\bar{p}_T)$.

4 Numerical experiments

In the following experiments, we measure the KL divergence values of distributions evolved through reverse SDEs and ODEs. We consider a simple data distribution p_0 , consisting of a mixture of Gaussians, for which the score functions $\nabla \log p_t$ can be analytically computed, and restrict ourselves to a one-dimensional setting for efficient entropy computation, as well as to allow direct visualization. Our consists of 10^5 samples of the Gaussian mixture distribution.

We focus on the EDM forward process [15], given by the SDE

$$dX_t = \sqrt{2t}dW_t. \quad (\text{EDM})$$

We also performed experiments with the Variance Exploding (VE) and Variance Preserving (VP) processes of [29], given by

$$dX_t = dW_t \quad (\text{VE})$$

$$dX_t = -\frac{1}{2}(\beta_1 t + \beta_2)X_t dt + \sqrt{\beta_1 t + \beta_2}dW_t, \quad (\text{VP})$$

and obtained qualitatively similar results, which can be found in Appendix C.

The functional parameter $\gamma(t)$ is taken as a constant γ , except at the end of Section 3.2, where it is set to a constant within a given interval $[S_{\min}, S_{\max}]$. Numerical integration is performed with Euler and Euler-Maruyama methods for ODEs and SDEs, respectively, using 500 discretization steps chosen according to the EDM time steps in [15], Table 1.

To avoid confusion, in this section we refer only to the forward time variable t , and consider the densities p_t and \tilde{p}_t in forward time. In this way, diffusion sampling starts at an 'initial time' $t = T$ and ends at a 'final time' $t = t_{\min}$, with $0 < t_{\min} < T$.

We compute relative entropies in two ways. The initial entropy $H(\tilde{p}_T|p_T)$, denoted by H_{init} , is obtained by numerical integration of the densities, which can be calculated analytically for the dataset considered. The final entropies $H(\tilde{p}_0|p_0)$, denoted by H_{ODE} and H_{SDE} , are computed from generated and data samples through the discretization of the empirical densities by an histogram of n_{bins} bins⁴. To reduce the dependence on the parameter n_{bins} , the entropies shown are the minimum of the values obtained for bins in the range $\{n_{\text{bins}} - 20, \dots, n_{\text{bins}}\}$. For our dataset, the precision of the entropy estimator was observed to be of the order of 5×10^{-4} .

⁴This estimator has limited precision, but we found it to be more reliable than the alternatives, such as using a KDE estimator for the densities or directly a non-parametric estimator for the entropies.

We calculate the bounds with the log-Sobolev constants obtained in [27]. The χ^2 -divergence for spherical Gaussians $\mu_0 \sim \mathcal{N}(m_0, \sigma_0^2 I)$ and $\mu_1 \sim \mathcal{N}(m_1, \sigma_1^2 I)$ has the closed form

$$\chi^2(\mu_0||\mu_1) = \left(\frac{2\sigma_0^2}{\sigma_1^2(\sigma_0^2 + \sigma_1^2/2)} \right)^{n/2} \exp\left(\frac{\|m_0 - m_1\|^2}{2\sigma_0^2 + \sigma_1^2} \right) - 1. \quad (25)$$

Then, from [27, Corollary 2] we know that the log-Sobolev constant for the Gaussian mixture $\mu_p = p\mu_0 + (1-p)\mu_1$ satisfies

$$C_p \leq \min(C_0, C_1), \quad (26)$$

with

$$\begin{aligned} C_0 &= \max\{\sigma_0^2(1 + (1-p)\lambda_p), \sigma_1^2(1 + p\lambda_p\chi_1)\} \\ C_1 &= \max\{\sigma_1^2(1 + p\lambda_p), \sigma_0^2(1 + (1-p)\lambda_p\chi_0)\}, \end{aligned}$$

where

$$\lambda_p := \begin{cases} 2 & , p = \frac{1}{2}, \\ \frac{\log p - \log(1-p)}{2p-1} & , p \neq \frac{1}{2}, \end{cases}$$

$$\chi_0 := \chi^2(\mu_0||\mu_1) + 1 \quad \text{and} \quad \chi_1 := \chi^2(\mu_1||\mu_0) + 1.$$

4.1 Analytical score functions

First, we generate distributions with analytical scores, in the setting of Section 3.1. We observe that our choice of final forward time T is taken artificially small, so that the entropy decrease is perceptible; we use $T = 0.75$ instead of the the default choice $T = 80$ [15], which would lead to a negligible initial entropy. Therefore, our approximate prior should not be seen as a tentative model of standard practice, but as an illustrative example of the phenomenon under study.

Figure 1 shows generated distributions and entropy evolution, sampling with analytical scores from the approximate prior at initial time T . We can see that the SDE induces a substantial decrease in the relative entropy, higher than ensured by our bound. The lack of tightness can be attributed to the log-Sobolev constant of p_t , which is valid for *any* q_t but used to a very specific $q_t = \tilde{p}_t$ which is close to p_t .

In Figure 2, we can see the effect of the initial time T on the final entropy, where the discretization grid is fixed and numerical integration initiated from an initial step i such that $t_i \approx T$. Note that SDE sampling produces smaller entropy values for a sufficiently large initial entropy value, associated with a smaller T . This effect is reduced when T is too small, which is expected since then there is not enough time for the stochastic correction to have an effect. The mismatch between initial entropy and final ODE entropy values is due to estimation errors for the latter, since by Theorem 1 they should be the same.

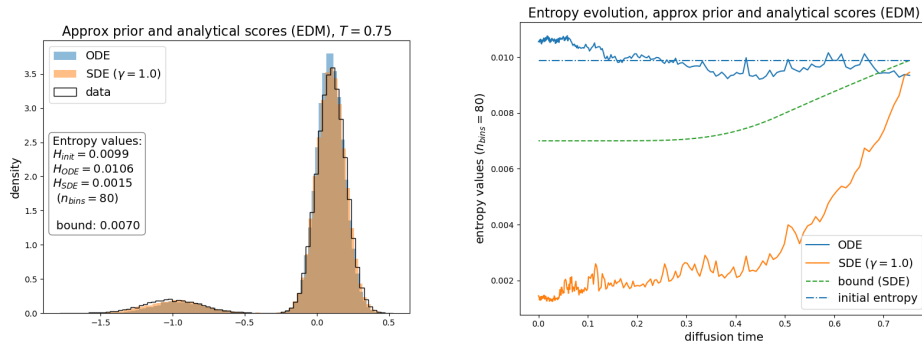


Figure 1: Data and generated distributions with analytical score functions (left) and entropy evolution (right).

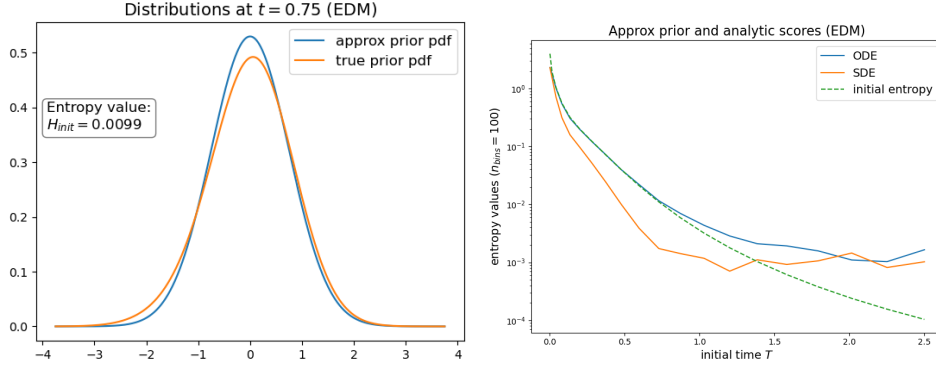


Figure 2: Prior error at a specific T (left) and the effect of initial time T on final entropy values (right).

Figure 3 shows the effect of γ and the number of discretization steps on the final entropy. In the left column, we can see that there is an optimal interval for γ for each choice of n_{steps} , and the right column shows that the increase in errors for large γ is associated with the "effective step size" for the Langevin part of the reverse SDE, given by $\gamma/n_{\text{steps}} \propto \gamma\Delta t$, as discussed in 3.1.1. In fact, equation (16) gives two "effective step sizes": $\Delta\tau_i$ for the Flow ODE part, in the first line, and $\gamma(\tau_i)\Delta\tau_i$ for the Langevin-like part in the second, but for large γ the errors from the second part clearly dominate.

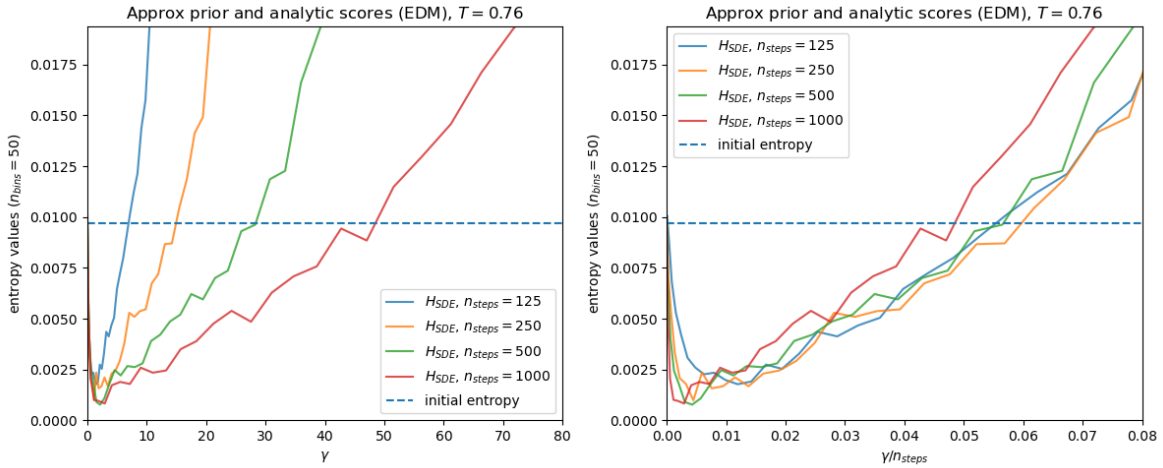


Figure 3: The effect of constant γ and discretization step size on final entropy. The horizontal axis on the right is the 'effective step size' described in 3.1.1.

4.2 Approximated score functions

Here, we sample with learned score functions, in the setting of Section 3.2. The score is approximated by a multi-layer-perceptron (MLP) of size [1000, 1000, 1000] with ReLU activations, trained by denoising score-matching. Figure 4 is the analog of Figure 1 for learned scores, where we also observe a lower entropy value for the SDE. The entropy evolution curves show an initial correction of the prior distribution error by the SDE, followed by the accumulation of score errors near the end of the sampling process. Since $\nabla \log h$ is unknown, we compute only the second bound of Theorem 4, equation (24), using an optimal $\delta(t)$ found by grid search.

More precisely, at each discretization step t_i we search for a $\delta(t_i)$ which minimizes the right-hand side of (40); since δ does not affect the quantities involved, choosing an optimal $\delta(t)$ at each time results in a minimal final bound. We show the rescaled version of this optimal $\delta(t)$, given by $d(t) := \delta(t)/\gamma(t)$, in bottom row of Figure 4, together with the expectation of the score errors $E_{\bar{p}}[\epsilon_t^2]$.

In addition, Figure 5 shows the results of sampling from exact prior distributions with learned

scores. Compared with Figure 4, we can see that the final entropies are similar for the SDE and lower for the ODE. Since in practice the final time T is chosen so that the prior approximation error is small, this setting can be seen as more realistic, and here the difference observed between SDE and ODE becomes very small. We found similar results experimenting with other datasets, often with a greater advantage for the SDE.

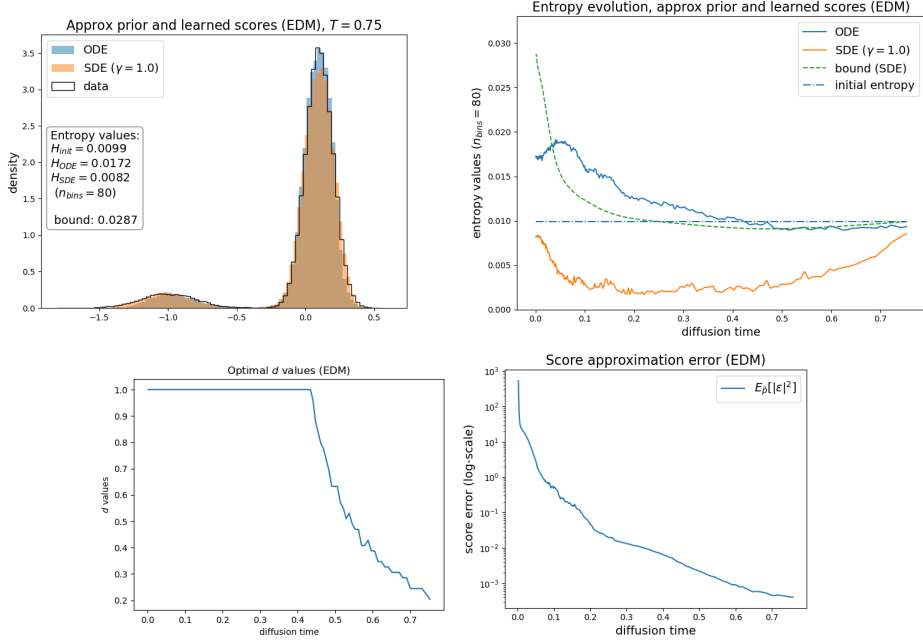


Figure 4: Generated distributions with approximate prior and learned score functions, and entropy evolution (top). Optimal $d(t) := \delta(t)/\gamma(t)g(t)^2$ and $L^2(\tilde{p}_t)$ -norm of the score error (bottom).

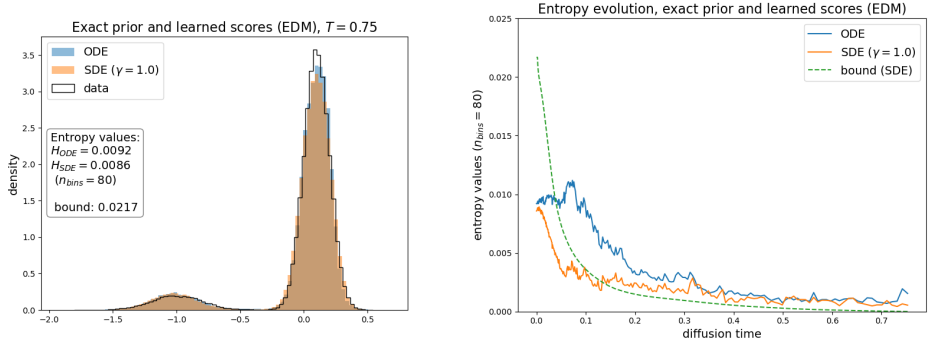
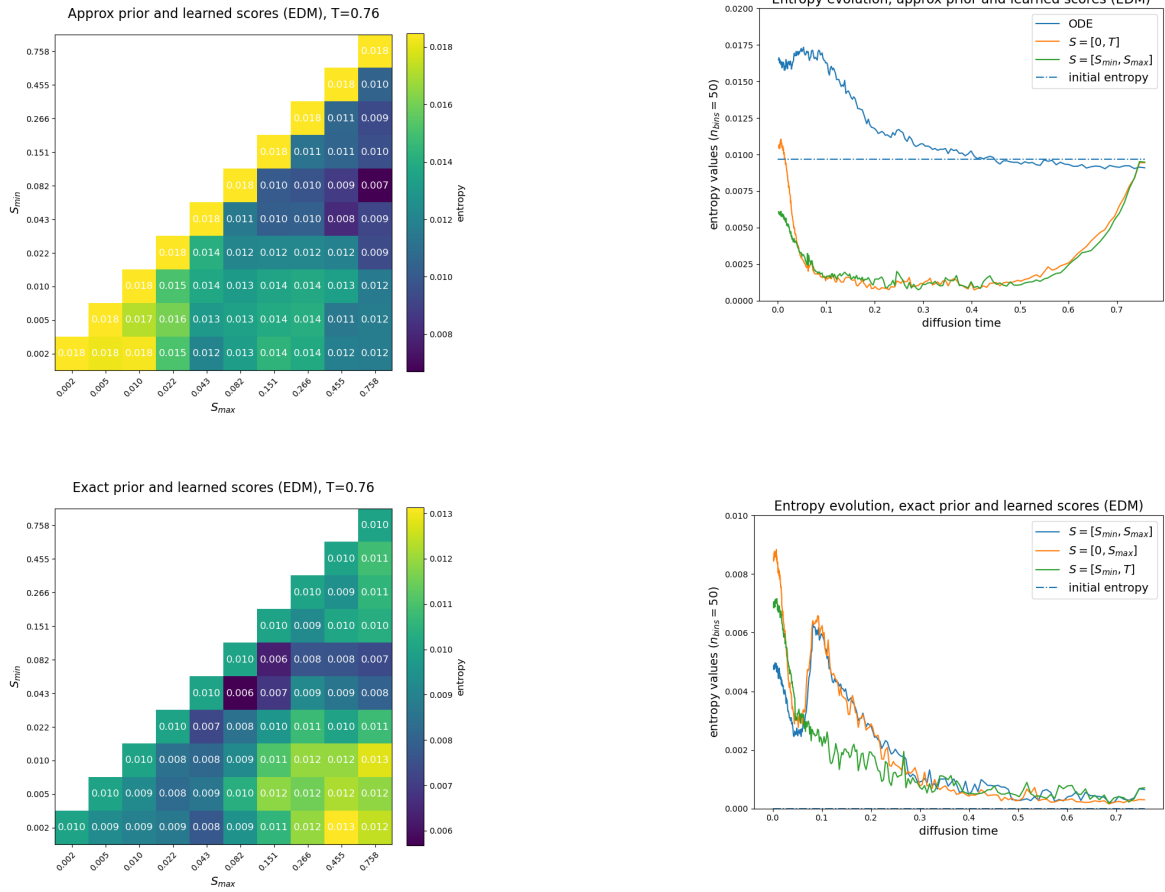


Figure 5: Generated distributions and entropy evolution, with exact prior and learned score functions.

Motivated by the previous entropy curves, Remark 3.2 and the observation that the score errors increase substantially for small t (Figure 4), we conjecture that stochasticity can be detrimental near $t = 0$. To test this, we set $\gamma(t) = 2$ for $t \in S = [S_{\min}, S_{\max}]$ and $\gamma(t) = 0$ otherwise, and vary the values of S_{\min} and S_{\max} within a fixed grid⁵. Figure 6a shows final entropy values for each interval, where the diagonal entries correspond to the pure ODE and the bottom right entry to the pure SDE. For an approximate prior setting $S_{\min} > t_{\min}$ leads to the lowest entropy, while for an exact prior setting $S_{\max} < T$ is also beneficial. This is consistent with Remark 3.2, since for an exact prior the initial accumulated error is too small to significantly affect $\nabla \log h_t(x)$.

⁵The idea of grid-searching for an optimal zone to introduce stochasticity in diffusion model sampling was previously done by [15] for CIFAR-10 images, using the Fréchet Inception Distance (FID) instead of KL divergence as the relevant metric. However, evolution curves are only possible if the metric can be computed for intermediary distributions, which is not the case for FID.

In Figure 6b, we can see the entropy evolution curve of the optimal choice of $[S_{\min}, S_{\max}]$, together with that of suboptimal choices, for comparison. Interestingly, comparing the cases of $S = [S_{\min}, T]$ with $S = [S_{\min}, S_{\max}]$ for the exact prior case, we see that introducing stochasticity before S_{\max} initially reduces the entropy, but induces an increase near the end, in the interval $[0, S_{\min}]$ where both equations are the same. Since in equations (19) and (23) the error contribution factor is given by the expectation of $\langle \nabla \log h_t, \epsilon_t \rangle$, this suggests that early stochasticity changes \tilde{p} in a way that the projection coefficient $\langle \nabla \log h_s, \epsilon_s \rangle$ is increased in average, for s close to 0⁶. This demonstrates one drawback of the heuristics proposed in Remark 3.2: the effects of the choice of $\gamma(t)$ can propagate to \tilde{p}_s for a very distant time $s \ll t$, limiting the usefulness of minimizing the derivative of $H(\tilde{p}_t|p_t)$ in $\gamma(t)$ independently for each t .



(a) Final entropy values, setting $\gamma(t) = 2$ for $t \in [S_{\min}, S_{\max}]$ and $\gamma(t) = 0$ otherwise.

(b) Entropy evolution for the optimal choices S_{\min}, S_{\max} from figure (a).

Figure 6: The effect of $\gamma(t)$ on relative entropies, sampling from approximate (top) and exact (bottom) prior with learned scores, for the EDM process.

Finally, Figure 7 shows the evolution of the relative entropy $H(p_t|\tilde{p}_t)$, instead of $H(\tilde{p}_t|p_t)$, together with the bound given in Corollary 3.2. Compared with Figure 4, we observe that the SDE produces a slightly larger decrease in this entropy, but the bound here is strictly crescent since it does not account for entropy decay. Although we cannot ensure that \tilde{p} satisfies an LSI, it might be true in this case, due to the structural similarity between \tilde{p}_t and p_t .

⁶In principle, we could use score-matching to estimate $\nabla \log \tilde{p}_t$, but the estimation error would be unknown.

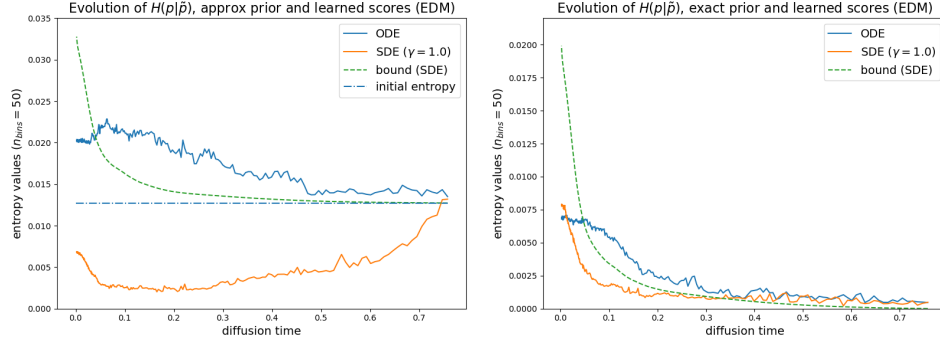


Figure 7: The evolution of the inverse entropy $H(p_t|\tilde{p}_t)$, together with the bound of Corollary 3.2, for the EDM process with learned score functions.

4.3 The effect of non-conservativity

In the ‘Practical considerations’ of [15, Section 4], it is suggested that detrimental effects of stochasticity could be attributed to the non-conservativity of the learned score. The previous experiments, however, show that the choice of the interval $S = [S_{\min}, S_{\max}]$ can make stochasticity detrimental even in a 1D setting, where every integrable function is conservative. Moreover, the KL divergence bounds obtained in Section 3.2 do not show an explicit effect of conservativity on error propagation.

To further investigate this point, we perform analogous experiments on a 2D Gaussian mixture dataset to see whether the negative effects of stochasticity are amplified. We found a similar qualitative behavior to the one-dimensional case, even though the learned score functions are not conservative in this case. We refer to Appendix B for more details. Based on this, it seems that conservativity by itself is not a crucial factor in the performance of stochastic sampling, although more nuanced effects could emerge in experiments with high-dimensional real-world data.

5 A fully analytic example

In this section, we consider an example for which we can explicitly compute the KL divergence and the first bound of Theorem 4, allowing a more direct analysis of the effect of the parameter γ . We start by assuming the ‘data’ distribution is a Gaussian $X_0 \sim \mathcal{N}(\mu_0, \sigma_0^2)$ and consider a forward equation of the form

$$dX_t = g(t)dW_t, \quad (27)$$

on a time interval $0 \leq t \leq T$, so the forward process is a Gauss-Markov process $X_t \sim \mathcal{N}(\mu_0, \sigma(t)^2)$, with score function

$$\nabla \log p(t, x) = -\frac{x - \mu_0}{\sigma(t)^2}, \quad \text{where } \sigma(t)^2 = \sigma_0^2 + \int_0^t g(s)^2 ds.$$

We then consider an approximate score of the form

$$s_\theta(t, x) = -\frac{x - \mu_\theta}{\sigma_\theta(t)^2}, \quad \sigma_\theta(t)^2 = \alpha_\theta \sigma(t)^2,$$

with constant parameters $\mu_\theta \in \mathbb{R}$ and $\alpha_\theta > 0$. The error to the exact score, defined in Section 3.2, becomes

$$\epsilon_t(x) = \frac{\mu_\theta(t) - \mu_0}{\sigma_\theta(t)^2} + \left(1 - \frac{\sigma(t)^2}{\sigma_\theta(t)^2}\right) \frac{x - \mu_0}{\sigma(t)^2}. \quad (28)$$

This approximate score yields the family of linear approximate reverse equations

$$d\tilde{X}_\tau = \frac{1}{2}\tilde{g}^2(\tau)(1 + \gamma(\tau)) \left(\frac{\tilde{X}_\tau - \tilde{\mu}_\theta(\tau)}{\tilde{\sigma}_\theta(\tau)^2} \right) d\tau + \sqrt{\gamma(\tau)}\tilde{g}(\tau)dW_\tau, \quad (29)$$

in the interval $0 \leq \tau \leq T$. Since this is a linear equation, it can be solved explicitly [14, Section 5.6], yielding the solution

$$\tilde{X}_\tau = e^{-A(\tau)} \tilde{X}_0 + e^{-A(\tau)} \int_0^\tau \bar{\mu}_\theta(s) a(s) e^{A(s)} ds + e^{-A(\tau)} \int_0^\tau \sqrt{\gamma(s)} \bar{g}(s) e^{A(s)} dW_s, \quad (30)$$

where

$$A(\tau) = \int_0^\tau a(s) ds, \quad a(\tau) = \frac{1}{2} \frac{\bar{g}(\tau)^2 (1 + \gamma(\tau))}{\bar{\sigma}_\theta(\tau)^2}.$$

Finally, we consider a prior, for the reverse process, which is also Gaussian, $\tilde{X}_0 \sim \mathcal{N}(\mu_T, \sigma_T^2)$. Thus, we obtain

$$\tilde{\mu}_\theta(\tau) = e^{-A(\tau)} \mu_T + e^{-A(\tau)} \int_0^\tau \bar{\mu}_\theta(s) a(s) e^{A(s)} ds \quad (31)$$

and

$$\tilde{\sigma}_\theta(\tau)^2 = e^{-2A(\tau)} \sigma_T^2 + e^{-2A(\tau)} \int_0^\tau \gamma(s) \bar{g}(s)^2 e^{2A(s)} ds. \quad (32)$$

For more explicit calculations, we further assume

$$\sigma_T^2 = \beta_T \sigma(T)^2, \quad \gamma(t) = \gamma. \quad (33)$$

so the free (constant) parameters for the sampling process are the shape-changing parameters $\alpha_\theta, \beta_T > 0$, the translation parameters $\mu_\theta, \mu_T \in \mathbb{R}$, the stochasticity parameter $\gamma \geq 0$, and the starting time $T > 0$. Besides these, we also have the parameters μ_0, σ_0, σ defining the forward distribution.

Then, the mean-square-error in the score becomes

$$\mathbb{E}_{\tilde{p}_\tau} [\tilde{\epsilon}_\tau^2] = \frac{(\mu_\theta - \mu_0)^2}{\alpha_\theta^2 \bar{\sigma}(\tau)^4} + \left(1 - \frac{1}{\alpha_\theta}\right)^2 \frac{1}{\bar{\sigma}(\tau)^2}. \quad (34)$$

Notice that, since the variance of the forward diffusion increases with time, the error in the score decreases, which coincides with the behavior in the numerical example, where the score is approximated by a neural network trained with denoising score-matching (see e.g. Figure 4).

With the parameters (33), the mean and variance of the Gauss-Markov approximate reverse process become

$$\tilde{\mu}_\theta(\tau) = \mu_\theta + \left(\frac{\bar{\sigma}(\tau)^2}{\bar{\sigma}(0)^2}\right)^{\frac{1}{2} \frac{(1+\gamma)}{\alpha_\theta}} (\mu_T - \mu_\theta). \quad (35)$$

and

$$\tilde{\sigma}_\theta(\tau)^2 = \begin{cases} \bar{\sigma}(\tau)^2 \left(\frac{\gamma \alpha_\theta}{(1+\gamma) - \alpha_\theta} + \left(\beta_T - \frac{\gamma \alpha_\theta}{(1+\gamma) - \alpha_\theta} \right) \left(\frac{\bar{\sigma}(\tau)^2}{\bar{\sigma}(0)^2} \right)^{\frac{(1+\gamma)}{\alpha_\theta} - 1} \right), & 1 + \gamma \neq \alpha_\theta, \\ \bar{\sigma}(\tau)^2 \left(\beta_T + \gamma \ln \left(\frac{\bar{\sigma}(0)^2}{\bar{\sigma}(\tau)^2} \right) \right), & 1 + \gamma = \alpha_\theta. \end{cases} \quad (36)$$

The KL divergence can be computed as

$$H(\tilde{p}_\tau | \tilde{p}_\tau) = \frac{1}{2} \left(\ln \frac{\bar{\sigma}(\tau)^2}{\bar{\sigma}_\theta(\tau)^2} + \frac{\bar{\sigma}_\theta(\tau)^2 + (\mu_0 - \tilde{\mu}_\theta(\tau))^2}{\bar{\sigma}(\tau)^2} - 1 \right). \quad (37)$$

In Figure 8, we can see the evolution of entropy and of the two bounds of Theorem 4, for a particular choice of prior and score errors, varying γ . Note that the second bound can, in some cases, be tighter than the first one, even though its derivation uses one further inequality. This is possible since the extra inequality is applied before the LSI (see Proof A.2).

Finally, Figure 9 shows the final KL divergence $H(\tilde{p}_0 | p_0)$, for many combinations of parameters. Even in this very simple example, we can see that the increase in γ can be beneficial or detrimental, depending on the initial condition and the score error. Interestingly, we can also see that the performance of the SDEs seems to be more stable to variations of the parameters.

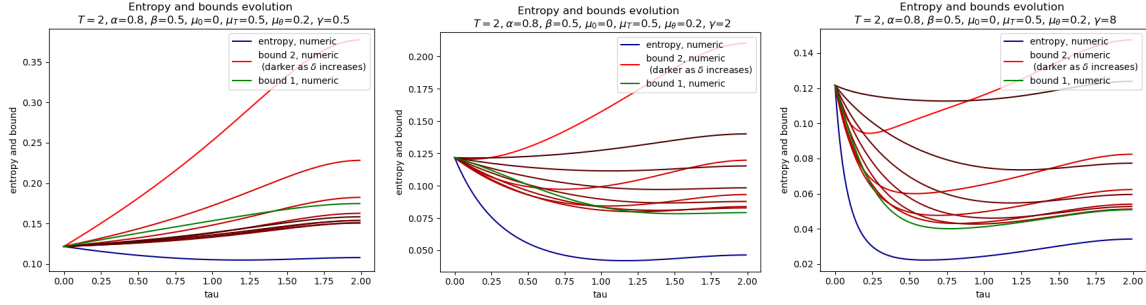


Figure 8: KL divergence and bounds evolution

Final KL divergence $H(\tilde{p}_0|\bar{p}_0)$ (EDM)

for assorted values of the parameters μ_θ , α_θ , β , and μ_T

■ $\gamma = 0.0$
■ $\gamma = 1.0$
■ $\gamma = 5.0$
■ $\gamma = 20.0$

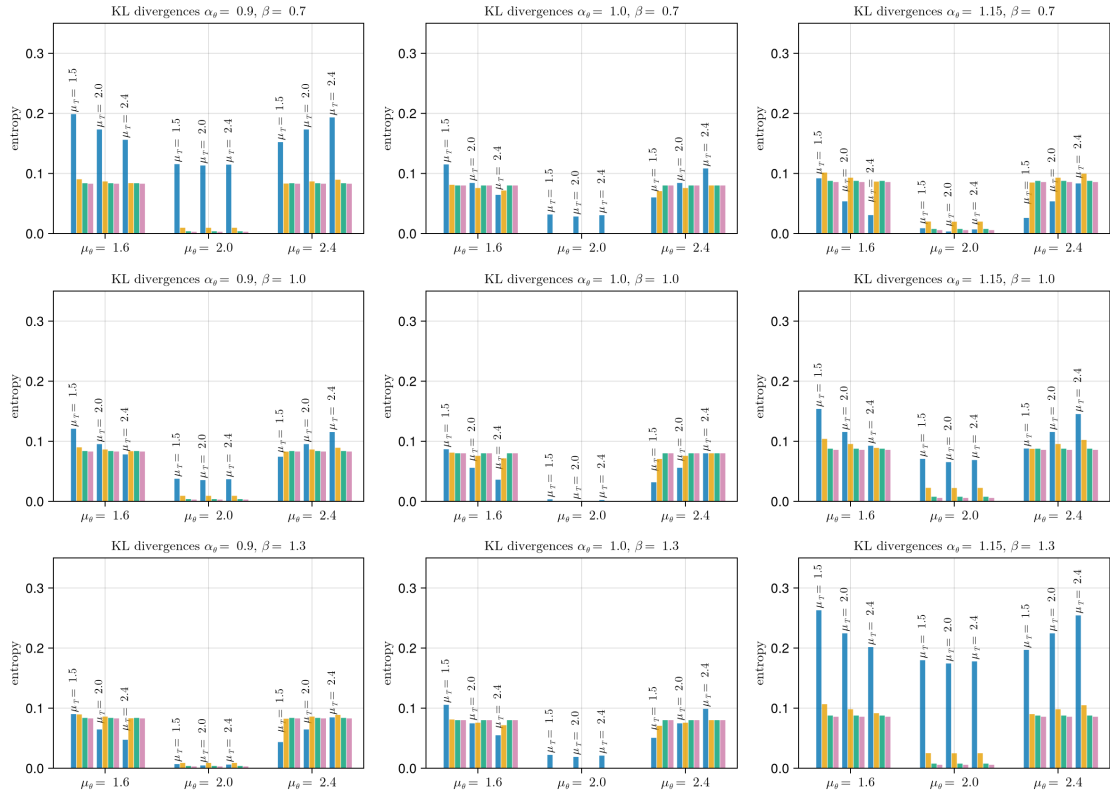


Figure 9: Final KL divergence $H(\tilde{p}_0|p_0)$ for $\gamma = 0.0, 1.0, 5.0, 20.0$, for various choices of the sampling parameters μ_θ , σ_θ , μ_T , and σ_T , with $\mu_0 = 2.0$, $\sigma_0 = 1.0$, $\sigma = 6.0$, and $T = 1.0$.

6 Conclusion

In this work, we studied differences between deterministic and stochastic sampling in diffusion models through KL divergence. Theorem 2 showed that a positive stochasticity parameter γ implies a reduction in the entropy between original and generated distributions, when considering exact score functions. One drawback of the bounds obtained is the dependence on log-Sobolev constants, whose optimal value can be difficult to obtain, and whose generality may lead to not so tight final bounds. This was observed for a simple dataset in Section 4. However, our result can be seen as a qualitative explanation of the error-correcting phenomenon observed in stochastic sampling.

The bound obtained for approximate scores offers a less clear interpretation, which is consistent

with the findings reported in the literature that stochastic sampling does not always lead to improved results [15]. The fact that $\nabla \log h_t$ gives a principal direction for error propagation, as observed in Remark 3.3, may be of further interest, along with the heuristics for choosing the stochasticity parameter $\gamma(t)$ suggested in Remark 3.2 and tested in our experiments.

Acknowledgment

The authors acknowledge the support of ExxonMobil Exploração Brasil Ltda. and Agência Nacional de Petróleo, Gás Natural e Biocombustíveis (ANP) through the grant no. 23789-1.

References

- [1] J. Abramson, J. Adler, J. Dunger, R. Evans, T. Green, A. Pritzel, O. Ronneberger, L. Willmore, A. Ballard, J. Bambrick, S. Bodenstein, D. Evans, C.-C. Hung, M. O’Neill, D. Reiman, K. Tunyasuvunakool, C. Wu, A. Žemgulytė, E. Arvaniti, and J. Jumper. Accurate structure prediction of biomolecular interactions with alphafold 3. *Nature*, 630:493–500, 05 2024.
- [2] M. S. Albergo, N. M. Boffi, and E. Vanden-Eijnden. Stochastic interpolants: A unifying framework for flows and diffusions, 2023.
- [3] B. D. Anderson. Reverse-time diffusion equation models. *Stochastic Process. Appl.*, 12(3): 313–326, 1982.
- [4] P. Bizeul. On the log-sobolev constant of log-concave measures [preprint], 2023. Available at <https://arxiv.org/abs/2306.12997>.
- [5] T. Brooks, B. Peebles, C. Holmes, W. DePue, Y. Guo, L. Jing, D. Schnurr, J. Taylor, T. Luhman, E. Luhman, C. Ng, R. Wang, and A. Ramesh. Video generation models as world simulators, 2024. Available at <https://openai.com/research/video-generation-models-as-world-simulators>.
- [6] H. Chen, H. Lee, and J. Lu. Improved analysis of score-based generative modeling: User-friendly bounds under minimal smoothness assumptions. In *International Conference on Machine Learning*, 2022.
- [7] H.-B. Chen, S. Chewi, and J. Niles-Weed. Dimension-free log-sobolev inequalities for mixture distributions. *Journal of Functional Analysis*, 281(11):109236, 2021.
- [8] S. Chen, S. Chewi, J. Li, Y. Li, A. Salim, and A. R. Zhang. Sampling is as easy as learning the score: theory for diffusion models with minimal data assumptions, 2023.
- [9] G. Conforti, A. Durmus, and M. G. Silveri. Kl convergence guarantees for score diffusion models under minimal data assumptions. *SIAM Journal on Mathematics of Data Science*, 7(1):86–109, 2025.
- [10] T. Deveney, J. Stanczuk, L. M. Kreusser, C. Budd, and C.-B. Schönlieb. Closing the ODE-SDE gap in score-based diffusion models through the Fokker-Planck equation [preprint], 2023. Available at <https://arxiv.org/abs/2311.15996>.
- [11] A. Figalli. Existence and uniqueness of martingale solutions for sdes with rough or degenerate coefficients. *Journal of Functional Analysis*, 254(1):109–153, 2008.
- [12] Z. Guo, J. Liu, Y. Wang, M. Chen, D. Wang, D. Xu, and J. Cheng. Diffusion models in bioinformatics and computational biology. *Nature Reviews Bioengineering*, 2(2):136–154, 2024.
- [13] M. Jiralerspong, A. J. Bose, I. Gemp, C. Qin, Y. Bachrach, and G. Gidel. Feature likelihood divergence: evaluating the generalization of generative models using samples. In *Proceedings of the 37th International Conference on Neural Information Processing Systems, NIPS ’23*, Red Hook, NY, USA, 2023. Curran Associates Inc.

- [14] I. Karatzas and S. E. Shreve. *Brownian Motion and Stochastic Calculus*. Springer-Verlag New York, 1988.
- [15] T. Karras, M. Aittala, T. Aila, and S. Laine. Elucidating the design space of diffusion-based generative models. *NeurIPS*, 2022. Available at <https://arxiv.org/abs/2206.00364>.
- [16] A. Kazerouni, E. K. Aghdam, M. Heidari, R. Azad, M. Fayyaz, I. Hacihaliloglu, and D. Merhof. Diffusion models for medical image analysis: A comprehensive survey, 2023. Available at <https://arxiv.org/abs/2211.07804>.
- [17] H. Lee, J. Lu, and Y. Tan. Convergence for score-based generative modeling with polynomial complexity, 2023.
- [18] W. Li, X. F. Cadet, D. Medina-Ortiz, M. D. Davari, R. Sowdhamini, C. Damour, Y. Li, A. Miranville, and F. Cadet. From thermodynamics to protein design: Diffusion models for biomolecule generation towards autonomous protein engineering, 2025. Available at <https://arxiv.org/abs/2501.02680>.
- [19] L. Lin, Z. Li, R. Li, X. Li, and J. Gao. Diffusion models for time series applications: A survey, 2023. Available at <https://arxiv.org/abs/2305.00624>.
- [20] P. A. Markowich and C. Villani. On the trend to equilibrium for the Fokker-Planck equation : An interplay between physics and functional analysis. 2004. Available at https://cedricvillani.org/sites/dev/files/old_images/2012/07/P01.MV-FPReview.pdf.
- [21] S. Menozzi, A. Pesce, and X. Zhang. Density and gradient estimates for non degenerate brownian sdes with unbounded measurable drift. *Journal of Differential Equations*, 272:330–369, 2021.
- [22] D. Naiff, B. P. Schaeffer, G. Pires, D. Stojkovic, T. Rapstine, and F. Ramos. Controlled latent diffusion models for 3d porous media reconstruction, 2025. Available at <https://arxiv.org/abs/2503.24083>.
- [23] I. Price, A. Sanchez-Gonzalez, F. Alet, T. R. Andersson, A. El-Kadi, D. Masters, T. Ewalds, J. Stott, S. Mohamed, P. Battaglia, R. Lam, and M. Willson. Gencast: Diffusion-based ensemble forecasting for medium-range weather, 2024. Available at <https://arxiv.org/abs/2312.15796>.
- [24] A. Ramesh, P. Dhariwal, A. Nichol, C. Chu, and M. Chen. Hierarchical text-conditional image generation with clip latents, 2022. Available at <https://arxiv.org/abs/2204.06125>.
- [25] G. O. Roberts and R. L. Tweedie. Exponential convergence of langevin distributions and their discrete approximations. *Bernoulli*, Vol. 2, No. 4. (Dec., 1996), pp. 341-363, 1996.
- [26] M. S. M. Sajjadi, O. Bachem, M. Lucic, O. Bousquet, and S. Gelly. Assessing generative models via precision and recall. In S. Bengio, H. Wallach, H. Larochelle, K. Grauman, N. Cesa-Bianchi, and R. Garnett, editors, *Advances in Neural Information Processing Systems*, volume 31. Curran Associates, Inc., 2018.
- [27] A. Schlichting. Poincaré and log-sobolev inequalities for mixtures. *Entropy*, 21(1), 2019. Available at <https://arxiv.org/pdf/1812.06464>.
- [28] Y. Song, C. Durkan, I. Murray, and S. Ermon. Maximum likelihood training of score-based diffusion models, 2021.
- [29] Y. Song, J. Sohl-Dickstein, D. P. Kingma, A. Kumar, S. Ermon, and B. Poole. Score-based generative modeling through stochastic differential equations. *In International Conference on Learning Representations (ICLR)*, 2021.
- [30] P. Vincent. A connection between score matching and denoising autoencoders. *Neural computation*, 23(7):1661–1674, 2011.
- [31] L. Yang, Z. Zhang, Y. Song, S. Hong, R. Xu, Y. Zhao, W. Zhang, B. Cui, and M.-H. Yang. Diffusion models: A comprehensive survey of methods and applications, 2024. Available at <https://arxiv.org/abs/2209.00796>.

- [32] C. Zhang, C. Zhang, S. Zheng, M. Zhang, M. Qamar, S.-H. Bae, and I. S. Kweon. A survey on audio diffusion models: Text to speech synthesis and enhancement in generative ai, 2023. Available at <https://arxiv.org/abs/2303.13336>.
- [33] H. Zou, Z. M. Kim, and D. Kang. A survey of diffusion models in natural language processing, 2023. Available at <https://arxiv.org/abs/2305.14671>.

A Proofs

A.1 Section 2

Below, we provide proofs of well known results, for the sake of completeness.

Proof of Lemma 2.1. We show that the Fokker-Planck equations associated with both SDEs are the same. Then, the uniqueness hypothesis on (4) ensures that its FP also has a unique solution [11], and thus the associated densities are the same.

To obtain formula (6), consider an arbitrary SDE in reverse-time τ , given by $d\hat{X}_\tau = a(\hat{X}_\tau, \tau)d\tau + b(\tau)dW_\tau$. Its FP equation is

$$\frac{\partial p_\tau}{\partial \tau} = -\nabla \cdot (ap_\tau) + \frac{1}{2}b^2\Delta p_\tau,$$

which, changing variables to $t := T - \tau$, becomes

$$\frac{\partial p_t}{\partial t} = \nabla \cdot (\bar{a}p_t) - \frac{1}{2}\bar{b}^2\Delta p_t, \quad (38)$$

with $\bar{a}(x, t) := a(x, T - t)$ and $\bar{b}(t) := b(T - t)$.

To find a and b such that the right-hand sides of (5) and (38) are the same, we can rewrite (5) as

$$\begin{aligned} \frac{\partial p}{\partial t} &= -\nabla \cdot (fp) + \frac{1}{2}g^2\Delta p \\ &= -\nabla \cdot (fp) + \frac{1}{2}g^2((1 + \gamma)\Delta p - \gamma\Delta p) \\ &= -\nabla \cdot (fp) + \frac{1}{2}g^2((1 + \gamma)(\nabla \cdot \nabla p) - \gamma\Delta p) \\ &= -\nabla \cdot (fp) + \frac{1}{2}g^2((1 + \gamma)(\nabla \cdot (p\nabla \log p)) - \gamma\Delta p) \quad \text{since } \nabla \log p = \frac{1}{p}\nabla p \\ &= \nabla \cdot \left(\left(-f + \frac{1}{2}g^2(1 + \gamma)\nabla \log p \right) p \right) - \frac{1}{2}g^2\gamma\Delta p, \end{aligned} \quad (39)$$

which is (38) for $\bar{a} = -f + \frac{1}{2}g^2(1 + \gamma)\nabla \log p$ and $\bar{b} = \sqrt{\gamma}g$. This gives exactly equation (6). \square

Proof of Lemma 2.2. If the Radom-Nikodym derivative $d\tilde{\mu}/d\mu$ is smooth, we can write $d\tilde{\mu} = f^2 d\mu$. Then, we have

$$\begin{aligned} \text{Ent}_\mu(f^2) &= \text{Ent}_\mu \left(\frac{d\tilde{\mu}}{d\mu} \right) = \int \frac{d\tilde{\mu}}{d\mu} \log \frac{d\tilde{\mu}}{d\mu} d\mu - \left(\int \frac{d\tilde{\mu}}{d\mu} d\mu \right) \log \left(\int \frac{d\tilde{\mu}}{d\mu} d\mu \right) \\ &= \int \log \frac{d\tilde{\mu}}{d\mu} d\tilde{\mu} - 1 \log 1 = H(\tilde{\mu}|\mu) \end{aligned}$$

and

$$\begin{aligned} \int \left\| \nabla \log \frac{\tilde{\mu}}{\mu} \right\|^2 d\tilde{\mu} &= \int \left\| \nabla \log f^2 \right\|^2 f^2 d\mu = \int \left\| \frac{1}{f^2} 2f\nabla f \right\|^2 f^2 d\mu \\ &= 4 \int \left\| \nabla f \right\|^2 d\mu. \end{aligned}$$

Therefore, if the LSI holds for μ , the second inequality also holds for all such $\tilde{\mu}$. \square

A.2 Section 3

Below, we prove our main results.

We observe that, although the statement of Lemma 3.1 can be found in [6, Lemma C.1], its proof there is purely formal. Here, we stated some sufficient regularity/integrability conditions for it, and provide a complete proof.

Proof of Lemma 3.1. As p_t and q_t are C^1 , we can differentiate under the integral sign to obtain

$$\begin{aligned} \frac{d}{dt}H(p_t|q_t) &= \int \partial_t \left(p_t(x) \log \frac{p_t(x)}{q_t(x)} \right) dx = \int \partial_t p_t \log \frac{p_t}{q_t} dx + \int \partial_t p_t dx - \int \frac{p_t}{q_x} \partial_t q_t dx \\ &= \int \partial_t p_t \log \frac{p_t}{q_t} dx - \int \frac{p_t}{q_t} \partial_t q_t dx =: I_1 + I_2, \end{aligned}$$

since $\int \partial_t p_t dx = d/dt \int p_t dx = 0$. Substituting the Fokker-Planck equation and integrating by parts, we have

$$I_1 = \int \nabla \cdot \left(a_1 p - \frac{1}{2} g^2 \nabla p \right) \log \frac{p_t}{q_t} dx = \int \left(a_1 p - \frac{1}{2} g^2 \nabla p \right) \cdot \nabla \log \frac{p}{q} dx$$

since $a_1 p \log(p/q)$ and $g^2(\nabla p) \log(p/q)$ are both $o(|x|^{n-1})$ by the hypotheses, and thus the boundary terms vanish at infinity. Analogously, we have

$$I_2 = - \int \nabla \cdot \left(a_2 p - \frac{1}{2} g^2 \nabla p \right) \frac{p}{q} dx = - \int \left(a_2 q - \frac{1}{2} g^2 \nabla q \right) \cdot \frac{p}{q} \nabla \log \frac{p}{q} dx$$

Using that $\nabla f = f \nabla \log f$, we can write

$$I_1 = \int p \left(a_1 - \frac{1}{2} g^2 \nabla \log p \right) \cdot \nabla \log \frac{p}{q} dx \quad \text{and} \quad I_2 = - \int p \left(a_2 - \frac{1}{2} g^2 \nabla \log q \right) \cdot \nabla \log \frac{p}{q} dx,$$

which gives

$$\begin{aligned} I_1 + I_2 &= \int p \left(a_1 - a_2 - \frac{1}{2} g^2 (\nabla \log p - \nabla \log q) \right) \cdot \nabla \log \frac{p}{q} dx \\ &= -\frac{1}{2} g^2 \int \left| \nabla \log \frac{p}{q} \right|^2 p dx + \int (a_1 - a_2) \cdot \nabla \log \frac{p}{q} p dx. \end{aligned}$$

□

Proof of Theorem 1. By Lemma 3.1, all we need to show is that these conditions ensure that ∇p_τ , \tilde{p}_τ and $\nabla \tilde{p}_\tau$ have super-polynomial decay at $x \rightarrow \infty$. The first is automatic because, as $\nabla \log p_\tau$ is Lipschitz, we have $\nabla p_\tau(x) = (\nabla \log p_\tau(x)) p_\tau(x) \leq C x p_\tau$.

The conditions for \tilde{p} follow from decay estimates for the fundamental solution of the Fokker-Planck equation [21, Theorem 1.2]. In general, if $p_t(x_t|x_0)$ is a fundamental solution of the FP equation of $dX_t = b(X_t, t)dt + \sigma(X_t, t)dW_t$ with σ Hölder and bounded, and b Lipschitz in x , then

$$|p_t(x_t|x_0)| \leq C_1 e^{-c_1 |x_t - \theta_t(x_0)|^2}$$

and

$$|\nabla_{x_t} p_t(x_t|x_0)| \leq C_2 e^{-c_2 |x_t - \theta_t(x_0)|^2},$$

where $C_1, c_1 > 0$ are constant in x , and θ is the deterministic flow associated with the drift, i.e.

$$\frac{d}{dt} \theta_t(x) = b(\theta_t(x), t), \quad \theta_0(x) = x.$$

In the particular case of equation (6), we have $\sigma(x, t) = \sigma(t)$ and the drift $b(x, t) := a(t) \nabla \log p_t(x)$, for some functions σ and a , and $|b(x, t)| \leq c_2(t)x + c_3(t)$ by the Lipschitz hypothesis on $\nabla \log p_t$. Hence, by Grönwall,

$$|\theta(x, t)| \leq |x_0| e^{\int_0^t c_2(s) ds} + e^{\int_0^t c_2(s) ds} \int_0^t c_3(s) ds =: a|x_0| + b.$$

Since $\tilde{p}_0(x_0) \sim \mathcal{N}(0, \sigma(T)I) = C_0 e^{-c_0|x_0|^2}$, we have

$$|\tilde{p}_t(x_t)| = \left| \int \tilde{p}_t(x_t|x_0)\tilde{p}_0(x_0)dx_0 \right| \leq \int C_2 e^{-(c_1|x-\theta_t(x_0)|^2+c_0|x_0|^2)} dx_0$$

for $C_2 := C_0 C_1$. Note that, for any $0 < \epsilon < 1$,

$$\begin{aligned} c_1|x-\theta_t(x_0)|^2+c_0|x_0|^2 &\geq \epsilon c_1(|x|^2-2\langle x,\theta_t(x_0)\rangle+|\theta_t(x_0)|^2)+c_0|x_0|^2 \\ &\geq \epsilon c_1\left(|x|^2-\frac{1}{2}|x|^2-2|\theta_t(x_0)|^2+|\theta_t(x_0)|^2\right)+c_0|x_0|^2 \\ &= \epsilon c_1\left(\frac{1}{2}|x|^2-|\theta_t(x_0)|^2\right)+c_0|x_0|^2 \\ &\geq \epsilon c_1\left(\frac{1}{2}|x|^2-(a|x_0|+b)^2\right)+c_0|x_0|^2 \\ &\geq \epsilon c_1\left(\frac{1}{2}|x|^2-2a^2|x_0|^2-2b^2\right)+c_0|x_0|^2 \\ &= \epsilon\frac{c_1}{2}|x|^2+(c_0-2\epsilon c_1 a^2)|x_0|^2-2\epsilon c_1 b^2 =: c_2|x|^2+c_3|x_0|^2+c_4. \end{aligned}$$

Taking $\epsilon < \min\left\{1, \frac{c_0}{2c_1 a^2}\right\}$, we have $c_3 > 0$, and thus

$$\begin{aligned} |\tilde{p}_t(x_t)| &\leq \int C_2 e^{-(c_1|x-\theta_t(x_0)|^2+c_0|x_0|^2)} dx_0 \leq \int C_2 e^{-(c_2|x|^2+c_3|x_0|^2+c_4)} dx_0 \\ &= C_2 e^{-(c_2|x|^2+c_4)} \int e^{-c_3|x_0|^2} dx_0 = C e^{-c|x|^2} \end{aligned}$$

for some constants $C, c > 0$. An exactly analogous argument shows the decay for $\nabla \tilde{p}_\tau$. \square

Proof of Corollary 3.1. The constant (15) is obtained in [7, Corollary 1]. To show that $\nabla \log p_t$ is Lipschitz in this case, denote the Gaussian pdf by

$$g_t(x) := \frac{1}{(2\pi t^2)^{\frac{1}{n}}} e^{-\frac{|x|^2}{2t^2}},$$

where $x \in \mathbb{R}^n$, and note that

$$\nabla \log p_t(x) = \frac{\nabla(p_0 * g_t)(x)}{p_t(x)} = \frac{p_0 * \nabla g_t(x)}{p_t(x)} = \frac{\int p_0(y) \frac{y-x}{t^2} g_t(x-y) dy}{p_t(x)} = \frac{1}{t^2} \left(-x + \frac{m_t(x)}{p_t(x)} \right),$$

where $m_t(x) := \int p_0(y) y g_t(x-y) dy$.

To see that $m_t(x)/p_t(x)$ is Lipschitz, note that $\nabla(m_t(x)/p_t(x))$ is bounded, since

$$\begin{aligned} \nabla \left(\frac{m_t(x)}{p_t(x)} \right) &= \frac{\nabla m_t(x)}{p_t(x)} - m_t(x) \frac{\nabla p_t(x)}{p_t(x)^2} \\ &= \frac{\frac{1}{t^2} \int p_0(y) y (y-x) g_t(x-y) dy}{p_t(x)} - m_t(x) \frac{\frac{1}{t^2} \int p_0(y) (y-x) g_t(x-y) dy}{p_t(x)^2} \\ &= \frac{1}{t^2} \left(\frac{\int p_0(y) y^2 g_t(x-y) dy}{p_t(x)} - \frac{x m_t(x)}{p_t(x)} - \frac{m_t(x)^2}{p_t(x)^2} + m_t(x) \frac{x}{p_t(x)} \right) \\ &= \frac{1}{t^2} \left(\frac{\int p_0(y) y^2 g_t(x-y) dy}{p_t(x)} - \frac{m_t(x)^2}{p_t(x)^2} \right) \\ &\leq \frac{1}{t^2} \left(\frac{\int p_0(y) R^2 g_t(x-y) dy}{p_t(x)} + \left(\frac{\int p_0(y) R g_t(x-y) dy}{p_t(x)} \right)^2 \right) = \frac{2R^2}{t^2}, \end{aligned}$$

using that $\text{supp } p_0 \subset B_R(0)$. \square

Proof of Theorem 4. 1. As in the proof of Theorem 2, using the log-Sobolev inequality (8) on the derivative of H , given by (19), we obtain

$$\frac{d}{ds} H(\tilde{p}_s | \bar{p}_s) \leq \frac{1}{2} g(s)^2 (1 + \gamma(s)) \int \epsilon_s \cdot (\nabla \log h_s) \tilde{p}_s dx - \frac{1}{C(s)} \gamma(s) g(s)^2 H(\tilde{p}_s | \bar{p}_s),$$

which, by Grönwall's inequality, gives

$$\begin{aligned} H(\tilde{p}_\tau | \bar{p}_\tau) &\leq \exp\left(-\int_0^\tau C(s)^{-1} \gamma(s) \bar{g}(s)^2 ds\right) H(\tilde{p}_0 | \bar{p}_0) \\ &\quad + \frac{1}{2} \int_0^\tau (1 + \gamma(s)) \bar{g}(s)^2 \left(\int \epsilon_s \cdot (\nabla \log h_s) \tilde{p}_s dx\right) \exp\left(-\int_s^\tau C(r)^{-1} \gamma(r) \bar{g}(r)^2 dr\right) ds. \end{aligned}$$

2. For the second claim, we wish to eliminate the unknown term $\nabla \log h_s$ from (19). Using Young's inequality, for any $\delta(s) > 0$ we have

$$\int \epsilon_t \cdot \nabla \log h_t \tilde{p}_t dx \leq \int |\epsilon_t| |\nabla \log h_t| \tilde{p}_t dx \leq \int \left(\frac{1}{4\delta_0(t)} |\epsilon_t|^2 + \delta_0(t) |\nabla \log h_t|^2\right) \tilde{p}_t dx,$$

where $\epsilon(\cdot, t)$ is square-integrable by the sub-Gaussian hypothesis. Then, if $\delta_0(s) \leq \gamma(s)/(\gamma(s)+1)$, by the LSI we have

$$\begin{aligned} \frac{d}{ds} H(\tilde{p}_s | \bar{p}_s) &\leq \frac{1}{8\delta_0} \bar{g}^2 (1 + \gamma) \int |\epsilon|^2 \tilde{p} dx - \frac{1}{2} \bar{g}^2 (\gamma - (\gamma + 1)\delta_0) \int \left|\nabla \log \frac{\tilde{p}}{\bar{p}}\right|^2 \tilde{p} dx \\ &\leq \frac{1}{8\delta_0} \bar{g}^2 (1 + \gamma) \int |\epsilon|^2 \tilde{p} dx - \frac{1}{C} \bar{g}^2 (\gamma - (\gamma + 1)\delta_0) H(\tilde{p} | \bar{p}). \end{aligned} \quad (40)$$

Taking $\delta = (\gamma + 1)\delta_0$ and using Grönwall inequality we obtain (24). \square

B 2D dataset

Here, we show analogous experiments on the 2D Gaussian mixture dataset shown in the top-left of Figure 10 to see whether the negative effects of stochasticity are amplified. In Figure 10 we can see a qualitative behavior similar to that of the one-dimensional case, even though the learned score functions are not conservative, as shown in Figure 10, bottom right, by the relative antisymmetry of the Jacobian $J = \nabla_x s_\theta(\cdot, t)$, given by

$$A(x, t) := \frac{\|J(x, t) - J^T(x, t)\|_F}{\|J(x, t)\|_F}, \quad (41)$$

averaged from 1000 samples of $x \sim p_t$ for each t , where $\|\cdot\|_F$ is the Frobenius norm.

C Other forward processes

Here, we present results from numerical experiments for the three processes analogous to those presented in Section 4 for the EDM process.

Exact prior and learned scores (EDM), $T = 0.80$

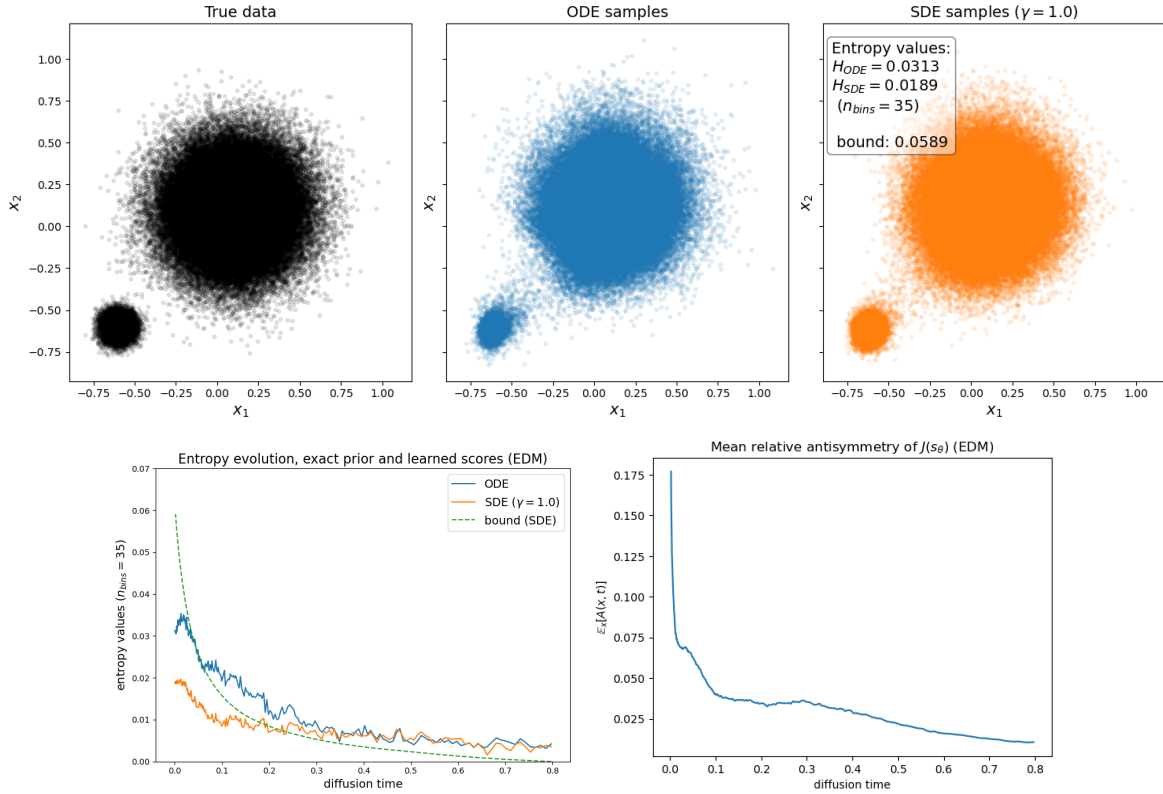


Figure 10: Generated distributions and entropy evolution for the EDM process, with exact prior and learned score functions for the 2D dataset.

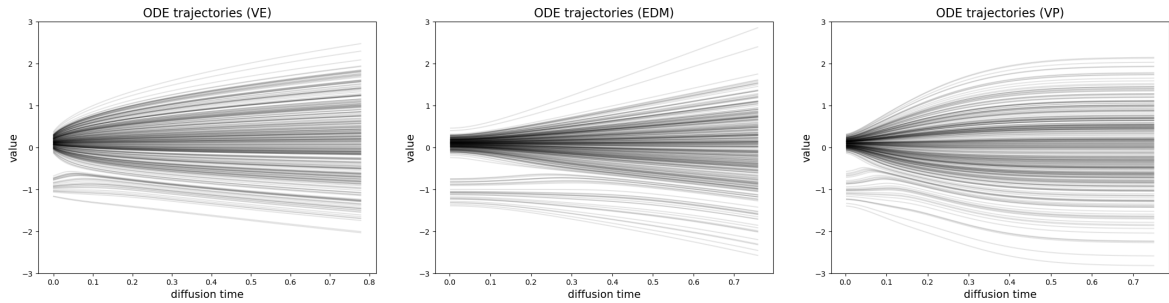


Figure 11: ODE trajectories with analytical scores for the three processes.

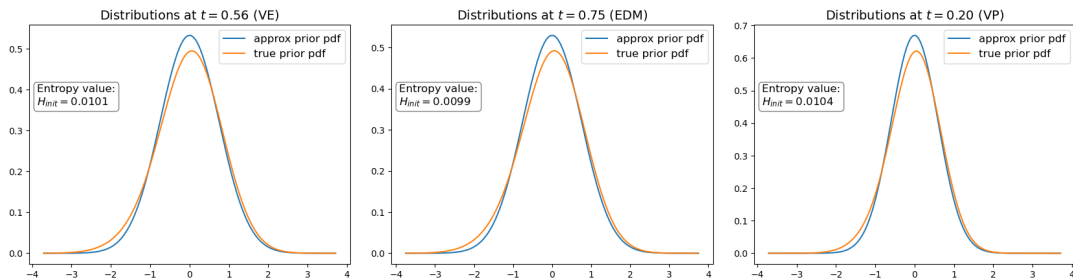


Figure 12: Approximate initial densities for the three processes.

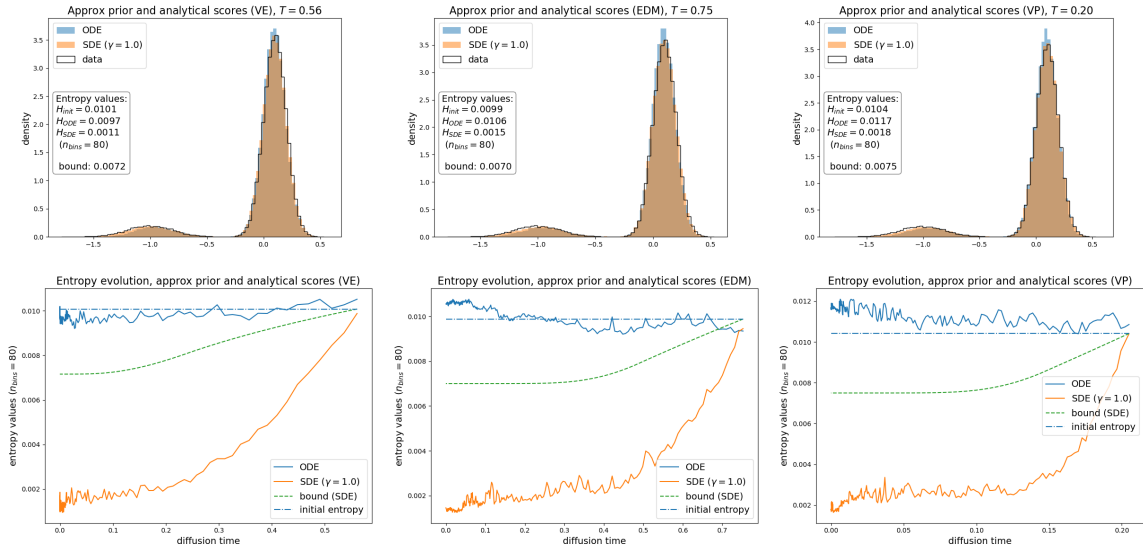


Figure 13: Data and generated distributions for the three processes, with analytical score functions, together with entropy evolution. Note that the horizontal axes have different time scales.

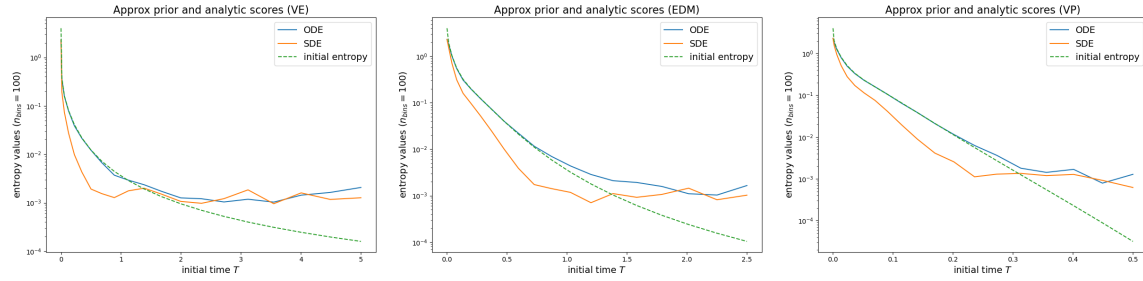


Figure 14: The effect of initial time T on final entropy values.

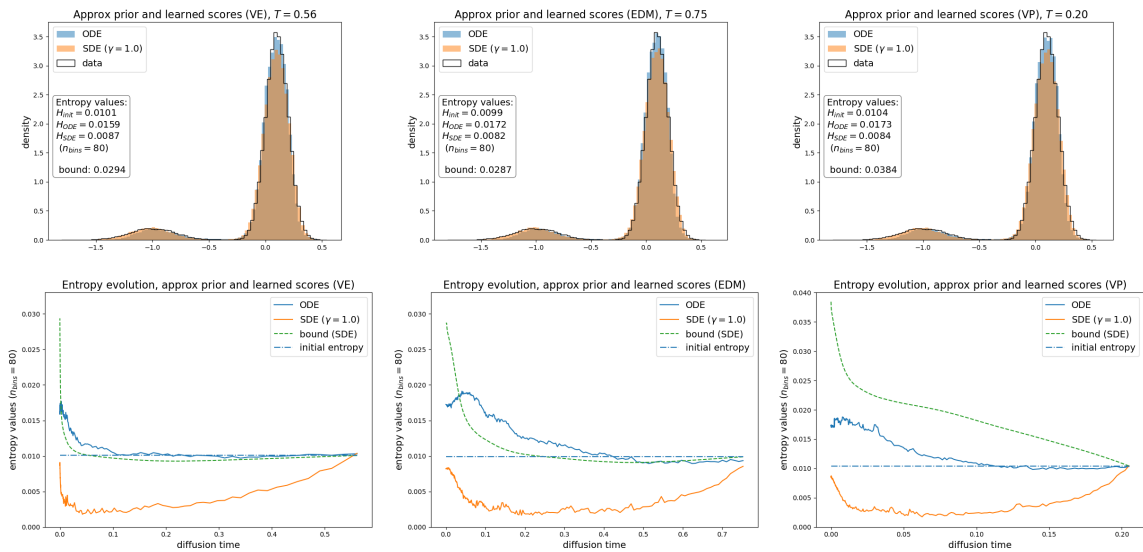


Figure 15: Generated distributions and entropy evolution for the three processes, with approximate prior and learned score functions.

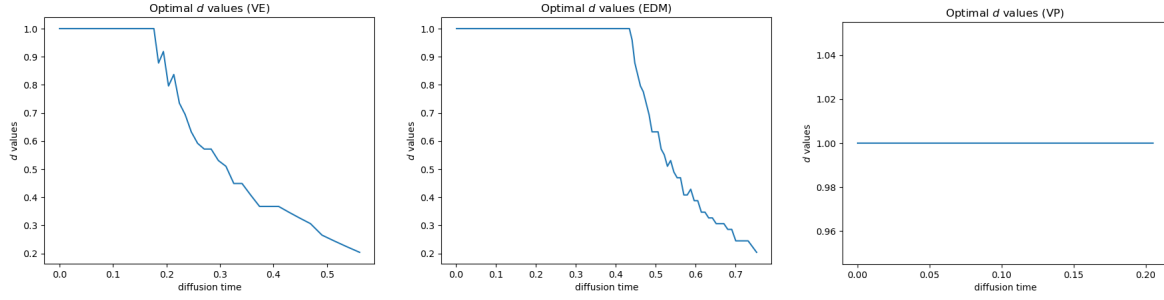


Figure 16: Optimal $d(t) := \delta(t)/\gamma(t)g(t)^2$ for the three processes, for the approximate prior.

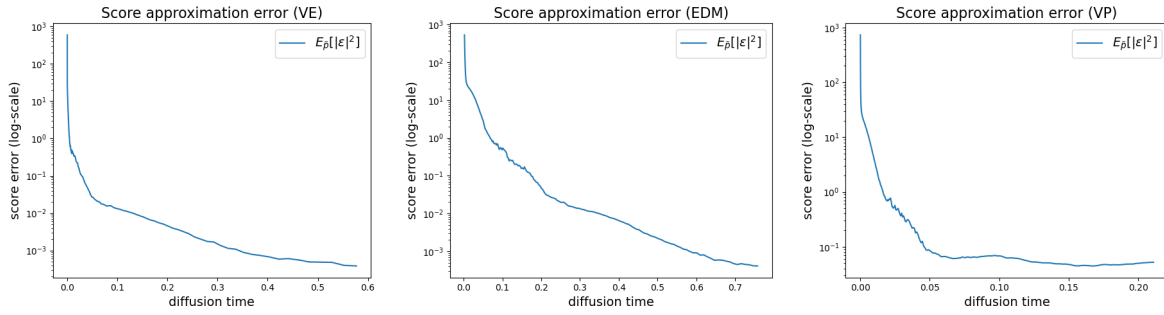


Figure 17: $L^2(\tilde{p}_t)$ -norm of the score error for the three processes, for the approximate prior.

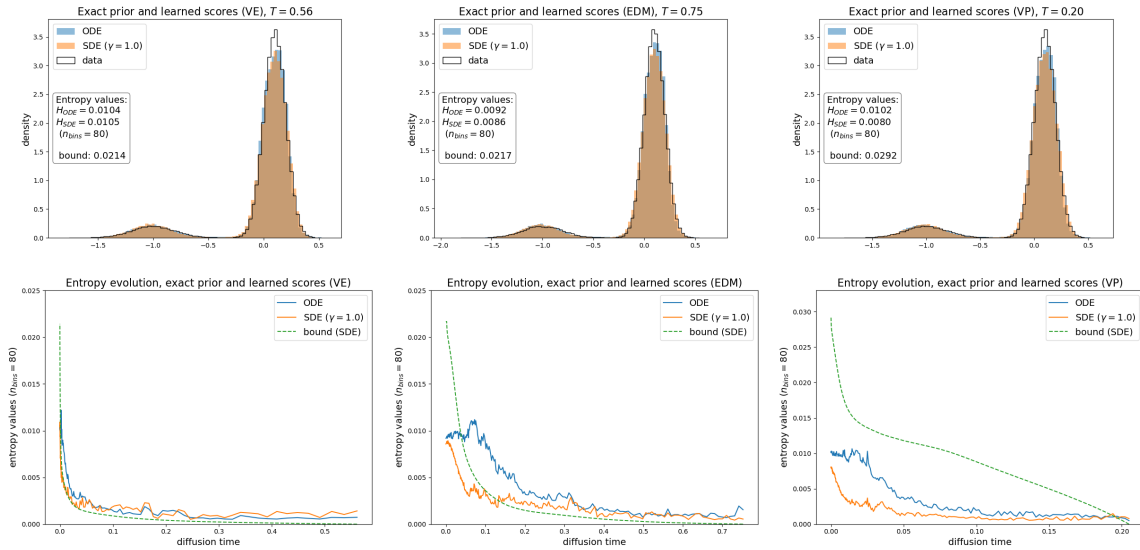


Figure 18: Generated distributions and entropy evolution for the three processes, with exact prior and learned score functions.